PREDICTION OF THE RESPONSE OF A CYLINDRICAL SHELL TO ARBITRARY OR BOUNDARY-LAYER-INDUCED RANDOM PRESSURE FIELDS

by

A.A. Lakis and M.P. Paidoussis

M.E.R.L. Report No. 72-2

March 1972

Department of Mechanical Engineering
McGill University
Montreal, P.Q., Canada

Summary

A general theory is presented for the response, to an arbitrary random pressure field, of a uniform or axially-non-uniform thin cylindrical shell. The theory is then specialized to the case where the pressure field originates from the turbulent boundary-layer of a subsonic internal flow.

The basic formulation of the dynamical problem is in terms of a hybrid classical/finite-element theory in which the finite elements are cylindrical frusta and the displacement functions are determined from the shell equations; the pressure forces are lumped at the nodes of the finite elements.

The cross-correlation spectral density and the mean square value of the displacements of the shell are obtained for an arbitrary pressure field and for a boundary-layer pressure field. Some calculations of the latter case are conducted to illustrate the theory. In one case the theory is compared with experiment, and agreement is found to be quite good.

CONTENTS

		Page
1.	INTRODUCTION	2
2.	MATRIX FORMULATION	6
2.1	Determination of the mass and stiffness matrices	7
2.2	Representation of continuous pressure field at nodal points	9
2.3	Decoupling of the equations	11
3.	RESPONSE TO ARBITRARY RANDOM PRESSURE FIELD	14
3.1	The mean square response in terms of the cross-correlation spectral density of the force field	14
3.2	The cross-correlation spectral densities of the force field	19
4.	RESPONSE TO BOUNDARY-LAYER PRESSURE FIELD	22
4.1	Dynamical effects of a flowing fluid	22
4.2	Longitudinal and lateral correlation functions	24
4.3	Mean square response	26
5.	CALCULATIONS AND DISCUSSION	32
6.	CONCLUSION	41
7.	ACKNOWLEDGEMENTS	44
APPENDIX:	Notation	45
REFERENCES		49
FIGURES 1 - 12		

1. INTRODUCTION

In this paper we are concerned with the vibration of thin circular cylindrical shells, either uniform or axially non-uniform, due to random pressure fields. A general theory is developed for predicting the response of such shells (i) to an arbitrary random pressure field and (ii) to a pressure field arising from the turbulent boundary layer of an internal subsonic flow.

Several theories are available for determining the response of beams and plates subjected to general, or boundary-layer excited, pressure fields, e.g. [1] - [7]. Considerably less attention has been paid to the case of cylindrical shells, inspite of the frequent occurrence of thin cylinders containing flow, or surrounded by axially flowing fluid, in industrial applications (including those in the more exotic fields of nuclear and space engineering). This reflects the added complexity of the problem in the case of cylindrical shells. To the authors' knowledge only two such studies have been made one by Cottis and Jasonides [8], and the other by Clinch [9].

The former is a general mathematical theory for simply-supported, uniform, thin cylindrical shells, based on Reissner's simplified, shallow shell, equations of motion. Using assumed correlation functions for the pressure field, Cottis and Jasonides derive a general expression for the space-time correlation of the response, for both arbitrary and boundary-layer induced pressure fields; but they do not proceed

to evaluate the mean square value of the response; moreover they do not undertake numerical solution of the problem. This work was later extended to orthotropic shells [10].

Clinch also considers simply-supported thin cylindrical shells which he analyses using Powell's [11] joint-acceptance method, essentially by-passing the need to introduce specific equations of motion. In the analysis he assumes that the areas over which the wall pressure fluctuations are correlated are small compared with pipe dimensions and, more importantly, considers the response only in the high modes of the shell (where resonances are so close to one another that a continuous curve of response versus frequency may be assumed). With these assumptions, and some others which are also made in [8] and in this paper, Clinch derives an expression for the root-mean-square of wall displacement essentially as a function of frequency bandwidth. He then compares his theoretical results to his own experimental data for a long and slender thin cylinder conveying water; the average r.m.s. wall displacement plotted against frequency displays remarkably good agreement between theory and experiment (in the range 100 - 1,000 Hz). It should also be added that Clinch obtained experimentally some very useful correlation functions for the pressure field.

A particularly attractive feature of Clinch's work from the application point of view, provided that the application falls within the limits of applicability of the theory,

is that one may calculate the r.m.s. response by performing a number of simple arithmetic calculations using several expressions and graphs in the paper. The most severe limitation of his theory is that it applies only for high mode numbers and frequencies.

The work presented in this paper is an attempt to produce a general theory for the response of cylindrical shells to random pressure fields, with a minimum of limitations and, hence, with wide range of applicability. It is based on a recently developed theory, [12] - [14], by the authors for the dynamical analysis of thin cylindrical shells.

The theory of [13], and hence the theory of this paper, is capable of analysing geometrically axially-symmetric, long or short, thin cylindrical shells which are not necessarily uniform, subject to any set of kinematic boundary conditions (including supports other than at the two axial extremities of the shell).

The specification of the random pressure field is first done in terms of quite general correlation functions, which are subsequently given special form appropriate for subsonic turbulent boundary layers; these latter correlation functions are taken from the existing literature [15, 9]. The assumption is made that the pressure field is spatially homogeneous and that it has the properties of a weakly stationary, ergodic process, as was done in both [8] and [9].

A number of other assumptions are also made which

are easiest understood when presented in the course of the analysis; a compendium of the assumptions and limits of applicability of the theory will be presented in the Conclusions.

The organization of the paper is as follows. First, the matrix formulation of the problem is presented, in the course of which the theory of [13] is outlined and the continuous pressure field is transformed to a discrete set of forces. Secondly, the cross-correlation spectral density and the mean square value of the shell are expressed in terms of correlation functions of the pressure field. Then, the special form of the theory for boundary-layer pressure fields is presented, and the root-mean-square of the response is obtained. Finally, the method of calculation is developed and the results of some calculations, conducted to illustrate the theory, are discussed.

2. MATRIX FORMULATION

We consider the dynamical behaviour of the shell subjected to arbitrary loads to be governed by the following equation

$$\underset{\sim}{M}\,\ddot{\underset{\sim}{y}} + \underset{\sim}{C}\,\dot{\underset{\sim}{y}} + \underset{\sim}{K}\,\underset{\sim}{y} = \underset{\sim}{F} \,, \tag{1}$$

where $\underset{\sim}{y}$ is a displacement vector, $\underset{\sim}{M}$, $\underset{\sim}{C}$ and $\underset{\sim}{K}$ are the mass, damping and stiffness matrices, respectively, and $\underset{\sim}{F}$ is a vector of the external forces. Thus, we have assumed that the continuum has been transformed to an equivalent discrete system with a finite number of degrees of freedom.

Whereas (1) is quite general, the particular form of its constituent terms depends on the particular theory used. In this paper we base our theory on a recently developed method for the analysis of axially non-uniform thin cylindrical shells [12] - [14], in which $\underset{\sim}{M}$ and $\underset{\sim}{K}$ were determined in order to obtain the free vibration characteristics of such shells. Only an outline of this theory is given here; for a detailed account the reader is referred to [13] or to [14].

The theory is a hybrid of the finite element and classical shell theories. The finite element chosen is a cylindrical frustum (Figure 1), and accordingly no geometrical modelling of the structure is necessary. Moreover, this allows us to use the shell equations, in full, for the determination of the displacement functions, instead of the more commonly used polynomial displacement functions.

2.1 DETERMINATION OF THE MASS AND STIFFNESS MATRICES

The displacement functions are determined by Sanders' theory [16, 17] for thin cylindrical shells. This shell theory was preferred, for the following reason: in Sanders' theory all strains vanish for small rigid-body motions, which is not true for Love's or Timoshenko's theories, for instance. By using such displacement functions we automatically satisfy the convergence criterion of the finite-element method stating that all strains within the element should vanish when the nodal displacements are generated by rigid-body motions.

In the continuum, we express the axial, circumferential and radial displacements of the middle surface of the shell by

$$\begin{aligned} U(x,\phi) &= \sum_n u_n(x) \cos n\phi, \\ V(x,\phi) &= \sum_n v_n(x) \sin n\phi, \\ W(x,\phi) &= \sum_n w_n(x) \cos n\phi, \end{aligned} \tag{2}$$

where u_n, v_n and w_n are the amplitudes of the displacements associated with the nth circumferential wavenumber. Then, <u>for a specific n</u>, the nodal displacement, say at node i (Figure 1), is defined by

$$\underset{\sim}{\delta}_i = \{u_{n_i}, w_{n_i}, (dw_n/dx)_i, v_{n_i}\}^T ; \tag{3}$$

for a finite element with nodes i and j, the nodal displacement vector is $\{\underset{\sim}{\delta}_i, \underset{\sim}{\delta}_j\}^T$.

Substituting (2) into Sanders' equations of equilibrium for the shell and proceeding according to the finite-element method [18], the displacement functions were determined [13] which relate the continuum displacement to the nodal displacements. Then the mass and stiffness matrices for one finite element, $\underset{\sim}{m}$ and $\underset{\sim}{k}$, respectively, were obtained analytically by carrying out the necessary matrix operations and integrations; after lengthy manipulation, expressions for the general terms k_{pq} and m_{pq} of $\underset{\sim}{k}$ and $\underset{\sim}{m}$ were obtained [12, 13]; these will not be reproduced here for the sake of brevity.

With $\underset{\sim}{m}$ and $\underset{\sim}{k}$ determined, the global mass and stiffness matrices for the whole shell, $\underset{\sim}{M}$ and $\underset{\sim}{K}$, respectively, may be constructed by superposition in the normal manner. Each of these (square) matrices is of order $4(N+1)$, where N is the total number of finite elements. The displacement vector $\underset{\sim}{y}$, for a shell subdivided into N finite elements, has the form

$$\underset{\sim}{y} = \{\underset{\sim}{\delta}_1, \underset{\sim}{\delta}_2, \cdots \underset{\sim}{\delta}_{N+1}\}^T. \tag{4}$$

It should be added that the analysis of reference [13] was extended in [19] for cases where the shell is fluid-filled, rather than in vacuo, essentially by modifying the mass matrix.

It must be stressed that, because of the form of equation (3), the mass and stiffness matrices obtained are associated with a specific n, as is the nodal displacement vector. Thus the analysis is carried out independently for each n.

2.2 REPRESENTATION OF CONTINUOUS PRESSURE FIELD AT NODAL POINTS

In equation (1) $\underset{\sim}{F}$ is quite general. In this paper all the external forces arise from an internal pressure field. It will be assumed that displacements are small enough for the resultant forces to be always normal to the shell. We shall now proceed to transform the continuous excitation field to a discrete set of forces acting at the nodal points.

It is well known that a set of forces on a rigid body may be represented by another set of forces acting at a different point, along with appropriate couples. The continuous random pressure field of the deformable body will be approximated here by a finite set of discrete forces and moments acting at the nodal points [20].

As previously mentioned, the shell is divided into N finite elements, each of which is a cylindrical frustrum. The position of the N+1 nodal points may be chosen arbitrarily (Figure 1).

Any pressure field is considered to be acting on an area S_e surrounding the node e of coordinate ℓ_e as shown in Figure 2a. This area S_e is delimited by the positions ℓ_e'' and ℓ_e' with respect to the origin in the x direction. It is therefore possible to approximate the pressure distribution acting over the area S_e by two mutually perpendicular forces per unit length. The forces $f_R(x,t)$ and $f_C(x,t)$ are at distance x_o from the origin of the shell as shown in Figure 2a; they

are given by

$$f_R(x,t) = r \int_0^{2\pi} p(x,\phi,t) \cos\phi \quad d\phi \ , \tag{5}$$

$$f_C(x,t) = r \int_0^{2\pi} p(x,\phi,t) \sin\phi \quad d\phi \ , \tag{6}$$

where $p(x,\phi,t)$ is the instantaneous pressure on the surface.

These two forces, f_R and f_C, acting at point A are transformed to two forces and one moment, m_r, acting at the node e, as shown in Figure 2b.

The external force vector at a typical node e can now be written in the following form:

$$\{F(t)\}_e = \begin{Bmatrix} 0 \\ \int_{\ell_i'}^{\ell_i''} f_R(x_i,t)\, dx_i \\ \int_{\ell_j'}^{\ell_j''} (x_j - \ell_j)\, f_R(x_j,t)\, dx_j \\ \int_{\ell_p'}^{\ell_p''} f_C(x_p,t)\, dx_p \end{Bmatrix}_e \tag{7}$$

where $\ell_i'' = \ell_j'' = \ell_p'' = \ell_e''$, $\ell_i' = \ell_j' = \ell_p' = \ell_e'$ and $\ell_e = \ell_j$, the peculiar indicial notation having been introduced for convenience in subsequent manipulations.

2.3 DECOUPLING OF THE EQUATIONS

All the terms in equation (1) have now been defined, except for $\underset{\sim}{C}$ which will not be given an explicit form for reasons to become obvious below. Before proceeding with the discussion of the response of the shell to random pressure fields, we shall discuss how the equations of motion may be decoupled, thereby defining a number of quantities which will be needed in the subsequent analysis.

To decouple the equations of motion we proceed by first considering the free vibration of the conservative system [13] and determining the eigenvalues and eigenvectors of the system. For a cylindrical shell subdivided into N finite elements where J kinematic boundary conditions have been imposed, the eigenvalue problem is of order $4(N+1)-J$. Here we consider that the natural frequencies, Ω_i, and the eigenvectors, $\underset{\sim}{\Phi}_i$, $i = 1, 2, \ldots 4(N+1)-J$, have been determined by the methods of [13].

We next form the modal matrix

$$\underset{\sim}{\Phi} = [\underset{\sim}{\Phi}_1, \underset{\sim}{\Phi}_2, \ldots \underset{\sim}{\Phi}_{4(N+1)-J}] , \tag{8}$$

and define

$$\underset{\sim}{y} = \underset{\sim\sim}{\Phi} \underset{\sim}{z} . \tag{9}$$

Substituting equation (9) into (1) and pre-multiplying by $\underset{\sim}{\Phi}^T$ we obtain

$$\underset{\sim\sim}{M}\ddot{\underset{\sim}{z}} + \underset{\sim\sim}{D}\dot{\underset{\sim}{z}} + \underset{\sim\sim}{S}\underset{\sim}{z} = \underset{\sim}{\Phi}^T\underset{\sim}{F} = \underset{\sim}{F}' , \tag{10}$$

where $\underset{\sim}{M}$ is the generalized mass matrix and $\underset{\sim}{S}$ is the spectral matrix, and they are both diagonal. $\underset{\sim}{D} = \underset{\sim}{\Phi}^T \underset{\sim}{C}\, \underset{\sim}{\Phi}$, on the other hand, is not diagonal, in general - albeit for small damping the off-diagonal terms are small and often negligible. Here we shall assume that $\underset{\sim}{C}$ is linearly related to $\underset{\sim}{M}$ and $\underset{\sim}{K}$, or to either one, in which case $\underset{\sim}{D}$ does become diagonal; moreover, we shall consider the case of hysteretic ('structural') damping to be a special case, from the point of view of mathematical representation, of the general viscous damping formulation adopted in equation (1). Denoting the rth (diagonal) term of $\underset{\sim}{D}$ by $D_r = 2\zeta_r (S_r M_r)^{1/2}$, S_r and M_r being the corresponding terms of $\underset{\sim}{S}$ and $\underset{\sim}{M}$, equation (10) leads to the decoupled set of equations

$$\ddot{z}_r + 2\zeta_r \Omega_r \dot{z}_r + \Omega_r^2 z_r = F_r' / M_r, \quad r = 1, 2, \ldots 4(N+1)-J \tag{11}$$

Upon solving equations (11), the response in terms of the original co-ordinates is found by

$$y_q = \sum_{r=1}^{4(N+1)-J} \Phi_{qr}\, z_r. \tag{12}$$

This then is the instantaneous response due to an arbitrary force vector $\underset{\sim}{F}$. We recall that it represents the response at the nodal points, i.e. at specific values of the co-ordinates x and ϕ, namely $x = x_i$, $i = 1, 2, \ldots N+1$, and $\phi = \phi_o$, where ϕ_o was defined consistently with $\underset{\sim}{F}$. Moreover, the response obtained above is associated with a specific n (section 2); by repeating the analysis for a sufficient number of n, the

total response for any point on the nodal circles may be obtained by superposition, using equation (2).

3. RESPONSE TO ARBITRARY RANDOM PRESSURE FIELD

Had the pressure field been deterministic, the response as expressed by (12) would have been the solution to the problem. In the case of a random field, however, we must proceed differently. In sections 3.1 and 3.2 we shall express the mean square of the response in terms of the spectral density of an arbitrary random pressure field, first in general terms (§3.1), and then using special forms of the spectral density of the pressure field (§3.2).

3.1 THE MEAN SQUARE RESPONSE IN TERMS OF THE CROSS-CORRELATION SPECTRAL DENSITY OF THE FORCE FIELD

The spatial cross-correlation function of the response is defined by

$$\psi_{y_{ij}}(x_k, x_p; \phi_o; \tau) = \overline{y_i(x_k,\phi_o,t)\, y_j(x_p,\phi_o,t+\tau)}, \qquad (13)$$

where y_i and y_j are two elements of the nodal displacement vector (it is recalled that y is a generic notation for u_n, v_n, w_n and dw_n/dx); x_k and x_p are the axial locations of the two nodes involved, where indices k and p are related to indices i and j, such that (for an unconstrained shell) to each k correspond four sequential values of i [equation (4)]; τ is the time delay and the bar denotes a time average.

Assuming that we are dealing with an ergodic process, using the correlation theorem, we may write

$$\psi_{y_{ij}}(x_k, x_p; \phi_o; \tau) = \lim_{T\to\infty} \frac{1}{4\pi T} \int_{-\infty}^{\infty} Y_i^*(x_k, \phi_o, \Omega, T)\, Y_j(x_p, \phi_o, \Omega, T) e^{i\Omega\tau} d\Omega, \tag{14}$$

where the Y's are the finite Fourier transforms of the y's, such that

$$Y_i(x_k, \phi_o, \Omega, T) = \int_{-T}^{T} y_i(x_k, \phi_o, t)\, e^{-i\Omega t}\, dt;$$

the asterisk denotes the complex conjugate. Now for $\tau=0$, and $i = j = q$, and hence $k = p = g$ (where q and g must be consistent), equations (13) and (14) may be written in the form

$$\overline{y^2_q(x_g, \phi_o, t)} = \psi_{y_{ij}}(x_g; \phi_o; 0)$$

$$= \lim_{T\to\infty} \frac{1}{2\pi T} \int_o^{\infty} Y_q^*(x_g, \phi_o, \Omega, T)\, Y_q(x_g, \phi_o, \Omega, T)\, d\Omega, \tag{15}$$

where the fact that $Y_q^* Y_q / 2T$ is an even function of Ω has been used.

Introducing the Fourier transforms of equations (11) and (12) into (15), we obtain

$$\overline{y^2_q(x_g, \phi_o, t)} = \sum_{r=1}^{4(N+1)-J} \sum_{s=1}^{4(N+1)-J} \frac{\Phi_{qr}\Phi_{qs}}{\Omega_r^2 \Omega_s^2 M_r M_s} \times$$

$$\times \lim_{T\to\infty} \frac{1}{2\pi T} \int_0^{\infty} e^{i(\theta_s - \theta_r)} |H_r(\Omega)||H_s(\Omega)| \underset{\sim}{\Phi}_r^T \underset{\sim}{F}(\Omega, T) \underset{\sim}{\Phi}_s^T \underset{\sim}{F}^*(\Omega, T)\, d\Omega, \tag{16}$$

where Ω_r is the rth natural frequency, M_r is the rth element

of the generalized mass matrix, Φ_{qr} is the qrth element of the modal matrix, θ_r and θ_s are phase lags between the force and the response, $H_r(\Omega)$ is the magnification factor defined by

$$H_r(\Omega) = \{[1 - (\frac{\Omega}{\Omega_r})^2]^2 + [2\zeta_r \frac{\Omega}{\Omega_r}]^2\}^{-1/2} ,$$

and $\underset{\sim}{F}(\Omega,T)$ is the finite Fourier transform of the force vector.

Figure 3 shows $|H_r(\Omega)|$ plotted against Ω for a lightly damped multi-degree-of-freedom system. We see that $|H_r(\Omega)|$ displays pronounced peaks in the neighbourhood of the natural frequencies of the system. The products $|H_r(\Omega)||H_s(\Omega)|$ for $r \neq s$ are seen to be small in comparison to the products for $r = s$. In addition, the terms in equation (16) with $r \neq s$ may be negative or positive depending on the sign of the product $\Phi_{qr}\Phi_{qs}$, while terms with $r = s$ are always positive. Therefore, the contribution of the cross-product terms to the mean square response will be small and may be ignored [21]. Equation (16) may now be written as

$$\overline{y_q^2}\,(x_g,\phi_o,t) = \sum_{r=1}^{4(N+1)-J} \frac{\Phi_{qr}^2}{\Omega_r^4 M_r^2} \times$$

$$\times \lim_{T\to\infty} \frac{1}{2\pi T} \int_0^\infty |H_r(\Omega)|^2 \underset{\sim}{\Phi}_r^T \underset{\sim}{F}(\Omega,T)\ \underset{\sim}{\Phi}_r^T \underset{\sim}{F}^*(\Omega,T)\ d\Omega. \quad (17)$$

We next define the cross-correlation spectral density of a force f by

$$W_f\,(x_i, x_j; \Omega; \tau=0) = \lim_{T\to\infty} [\frac{1}{T} F(x_i,\Omega,T)\ F^*(x_j,\Omega,T)] \quad (18)$$

where F is the Fourier transform of f. Substituting the Fourier transform of equation (7) into (17), expanding and making use of equation (18), we obtain

$$\overline{y_q^2(x_g,\phi_o,t)} = \sum_{r=1}^{4(N+1)-J} \frac{\phi_{qr}^2}{2\pi\Omega_r^4 M_r^2} \int_0^\infty |H_r(\Omega)|^2 \times$$

$$\times \left\{ \sum_{i=1}^{N+1}\sum_{u=1}^{N+1} \Phi_{ir}\Phi_{ur} \left| \int_{\ell_i'}^{\ell_i''} \int_{\ell_u'}^{\ell_u''} W_{f_R}(\Omega; x_i, x_u; 0)\, dx_i\, dx_u \right| \right.$$

$$+ \sum_{i=1}^{N+1}\sum_{k=1}^{N+1} \Phi_{ir}\Phi_{kr} \left| \int_{\ell_i'}^{\ell_i''} \int_{\ell_k'}^{\ell_k''} (x_k-\ell_k)\, W_{f_R}(\Omega; x_i, x_k; 0)\, dx_i\, dx_k \right|$$

$$+ \sum_{i=1}^{N+1}\sum_{v=1}^{N+1} \Phi_{ir}\Phi_{vr} \left| \int_{\ell_i'}^{\ell_i''} \int_{\ell_v'}^{\ell_v''} W_{f_{RC}}(\Omega; x_i, x_v; 0)\, dx_i\, dx_v \right|$$

$$+ \sum_{j=1}^{N+1}\sum_{u=1}^{N+1} \Phi_{jr}\Phi_{ur} \left| \int_{\ell_j'}^{\ell_j''} \int_{\ell_u'}^{\ell_u''} (x_j-\ell_j)\, W_{f_R}(\Omega; x_j, x_u; 0)\, dx_j\, dx_u \right|$$

$$+ \sum_{j=1}^{N+1}\sum_{k=1}^{N+1} \Phi_{jr}\Phi_{kr} \left| \int_{\ell_j'}^{\ell_j''} \int_{\ell_k'}^{\ell_k''} (x_j-\ell_j)(x_k-\ell_k)\, W_{f_R}(\Omega; x_j; x_k; 0)\, dx_j\, dx \right.$$

$$+ \sum_{j=1}^{N+1}\sum_{v=1}^{N+1} \Phi_{jr}\Phi_{vr} \left| \int_{\ell_j'}^{\ell_j''} \int_{\ell_v'}^{\ell_v''} (x_j-\ell_j)\, W_{f_{RC}}(\Omega; x_j, x_v; 0)\, dx_j\, dx_v \right|$$

$$+ \sum_{p=1}^{N+1}\sum_{u=1}^{N+1} \Phi_{pr}\Phi_{ur} \left| \int_{\ell_p'}^{\ell_p''} \int_{\ell_u'}^{\ell_u''} W_{f_{CR}}(\Omega; x_p, x_u; 0)\, dx_p\, dx_u \right| \qquad (19)$$

$$+ \sum_{p=1}^{N+1}\sum_{k=1}^{N+1} \Phi_{pr}\Phi_{kr} \left| \int_{\ell_p'}^{\ell_p''} \int_{\ell_k'}^{\ell_k''} (x_k-\ell_k)\, W_{f_{CR}}(\Omega; x_k, x_p; 0)\, dx_p\, dx_k \right|$$

$$+ \sum_{p=1}^{N+1} \sum_{v=1}^{N+1} \Phi_{pr}\Phi_{vr} \left| \int_{\ell_p'}^{\ell_p''} \int_{\ell_v'}^{\ell_v''} W_{f_C}(\Omega;\, x_p, x_v;\, 0)\, dx_p\, dx_v \right| \Bigg\} d\Omega,$$

where W_{f_R} and W_{f_C} are forms of (18) involving the forces f_R and f_C, respectively, and $W_{f_{RC}}$ and $W_{f_{CR}}$ represent mixed terms involving both f_R and f_C [see also equation (23)]. In the above equation the indices i and u are associated with radial forces, p and v with circumferential forces, and j and k with moments.

3.2 THE CROSS-CORRELATION SPECTRAL DENSITIES OF THE FORCE FIELD

The cross-correlation spectral density, W_f, of a force field, $f(x,t)$, may be obtained experimentally, in principle, by multiplying electronically $f(x_s,t)$ and $f(x_k,t)$ after passing them through identical narrow-band filters with central frequency Ω, and taking a long time average. Thus

$$W_f(x_s, x_k; \Omega; 0) = \overline{f_\Omega(x_s,t)\ f_\Omega(x_k,t)} \ . \tag{20}$$

Now, if the force field is derived from a homogeneous pressure field, the cross-correlation spectral density of both the pressure and the force fields may be expressed in terms of distances of separation $\xi=|x_s-x_k|$ and $\eta=|r(\phi_i-\phi_j)|$, instead of the co-ordinates themselves. Thus, we have

$$\overline{p_\Omega(x_s,\phi_i,t)\ p_\Omega(x_k,\phi_j,t)} = \overline{p_\Omega(x,\phi,t)\ p_\Omega(x+\xi,\phi+\eta,t)}, \tag{21}$$

and

$$\overline{f_\Omega(x_s,t)\ f_\Omega(x_k,t)} = \overline{f_\Omega(x,t)\ f_\Omega(x+\xi,\ t)}. \tag{22}$$

In this paper the pressure field is related to the components of the force field f_R and f_C through equations (5) and (6). Accordingly, the cross-correlation spectral densities employed in equation (19) may now be written as follows:

$$W_{f_R}(\xi,\Omega,0) = \overline{f_{R_\Omega}(x,t)\ f_{R_\Omega}(x+\xi,\ t)}$$

$$= r^2 \int_0^{2\pi}\int_0^{2\pi} \overline{p_\Omega(x,\phi,t)\ p_\Omega(x+\xi,\phi+\eta,t)}\cos\phi\cos(\phi+\eta)\ d\phi d(\phi+\eta),$$

$$W_{f_C}(\xi,\Omega,0) = \overline{f_{C_\Omega}(x,t)\ f_{C_\Omega}(x+\xi,t)}$$

$$= r^2 \int_0^{2\pi}\int_0^{2\pi} \overline{p_\Omega(x,\phi,t)\ p_\Omega(x+\xi,\phi+\eta,t)}\ \sin\phi\ \sin(\phi+\eta)\ d\phi d(\phi+\eta), \tag{23}$$

$$W_{f_{RC}}(\xi,\Omega,0) = \overline{f_{R_\Omega}(x,t)\ f_{C_\Omega}(x+\xi,t)}$$

$$= r^2 \int_0^{2\pi}\int_0^{2\pi} \overline{p_\Omega(x,\phi,t)\ p_\Omega(x+\xi,\phi+\eta,t)}\cos\phi\sin(\phi+\eta)d\phi d(\phi+\eta),$$

and

$$W_{f_{CR}}(\xi,\Omega,0) = W_{f_{RC}}.$$

Thus the W_f's, and hence the response of the shell [through equation (19)], will be determined once the quantity $\overline{p_\Omega(x,\phi,t)p_\Omega(x+\xi,\phi+\eta,t)}$ is specified.

We introduce the normalized spatial cross-correlation function for the pressure field

$$\psi_p(\xi,\eta,\tau) = \frac{\overline{p(x,\phi,t)\ p(x+\xi,\phi+\eta,t+\tau)}}{\overline{p^2(x,\phi,t)}} \tag{24}$$

where $\overline{p^2(x,\phi,t)} \equiv \overline{p^2(t)}$ is the mean square of the pressure fluctuations. It will be assumed that we can write $\psi_p(\xi,\eta,0) = \psi_p(\xi,0,0)\ \psi_p(0,\eta,0)$. The quantities $\psi_p(\xi,0,0)$ and $\psi_p(0,\eta,0)$, which are, respectively, the axial and circumferential spatial correlation functions, may be determined experimentally with relative ease; by a procedure such as that outlined at the beginning of this section we may obtain these values of ψ_p for

specific frequency bands, which we denote by ψ_{p_Ω}. Accordingly, equation (24) may be re-written in the form

$$\overline{p_\Omega(x,\phi,t)\ p_\Omega(x+\xi,\phi+\eta,t)} = \psi_{p_\Omega}(\xi,0,0)\ \psi_{p_\Omega}(0,\eta,0)\ \overline{p^2{}_\Omega(t)} \qquad (2$$

Equations (25) and (23) express the spectral cross-correlations of the force field in terms of the pertinent correlation of the pressure field. Thus equations (25), (23) and (19) together express the response of the shell to an arbitrary homogeneous random pressure field.

4. RESPONSE TO BOUNDARY-LAYER PRESSURE FIELD

In the previous section we obtained expressions for the response of a shell subjected to an arbitrary random pressure field. The origin of the pressure field was left undefined. Here we shall consider the particular case where the pressure field arises from pressure fluctuations in the subsonic, turbulent boundary layer of a fluid flowing inside the shell.

4.1 DYNAMICAL EFFECTS OF A FLOWING FLUID

In reference [19] we have indicated how the inertial effects of a stationary fluid contained by the shell may be taken into account. However, when the fluid is flowing, there are additional factors that must be considered, in connection with the effect of the mean flow on the dynamics of the system. Thus the shell will be subjected to 'centrifugal' forces proportional to $\bar{U}^2(\partial^2 w/\partial x^2)$ and Coriolis-type forces proportional to $2\bar{U}(\partial^2 w/\partial x \partial t)$, where $\bar{U}$ is the mean flow velocity [21], [22]. In broad terms, the former have the effect of diminishing the natural frequencies of the system, while the latter have a damping effect on vibrations in cases where one end of the shell is free - at least at flow velocities that are not near to, or above, those at which instabilities take place [21]. The magnitude of these effects depends on the dimensionless flow velocity $\mathcal{U} = \bar{U}\,[(1-\nu^2)\rho/E]^{1/2}$. Unless we are dealing with very flexible (e.g. rubber) shells, very heavy fluids, or very high flow velocities, the value of $\mathcal{U}$ will be small and the effect

of these forces will be correspondingly small. Thus, for a steel cylindrical shell with $L/r = 26$ and $t/r = 0.023$ conveying air-flow, $\mathcal{U} = 0.20$ corresponds to $\bar{U} = 3{,}330$ ft/sec.; for this magnitude of flow velocity, which is really beyond the range we shall be considering, the natural frequencies of the shell (clamped at both ends) are found to diminish by only 3% as a result of the flow. Accordingly, for metal tubes conveying fluid with flow velocity in the normal engineering range, these effects are negligible and will not be taken into account in this paper.

It is also assumed that the internal pressures are not unduly high, so that pressurization of the shell is negligible. We further assume that pressure drop in the length of the shell is sufficiently small for the mean pressure to be considered constant over the length of the shell (thus excluding very long, slender shells); this, however, is not a limitation of the theory, but a simplification introduced for convenience.

Finally, in this section we exclude the effect of random pressure disturbances other than from a boundary layer; this also is not a limitation of the theory, as composite random pressure fields may always be analysed by the methods of §3.

4.2 LONGITUDINAL AND LATERAL CORRELATION FUNCTIONS

In the case of subsonic boundary-layer pressure fluctuations, the streamwise and lateral spatial correlation functions have been examined theoretically and experimentally by several investigators [24] - [30].

Bakewell [15, 28] measured, and derived expressions for, the axial and circumferential correlation functions, in experiments with air flowing in a cylindrical pipe. The experiments covered a range of Reynolds numbers from 10^5 to 3×10^5.

We denote the axial and circumferential correlation functions per unit band-width with centre frequency ω by $\psi_{p_\omega}(\xi,0,0)$ and $\psi_{p_\omega}(0,\eta,0)$, respectively; the subscript ω is now used instead of Ω to indicate that the centre frequency is in Hz and not in rad/sec; (in this section we shall be using expressions with numerical constants, so the distinction is important). Bakewell found [28] that his experimental points defined the following approximate expressions for the spatial correlations:

$$\psi_{p_\omega}(\xi,0,0) \simeq e^{-b|S_\xi|}\cos a S_\xi \tag{26}$$

$$\psi_{p_\omega}(0,\eta,0) \simeq (1+c\, S_\eta^2)^{-1}\,[2 - e^{-dS_\eta^2}]^{-1} \tag{27}$$

where $S_\xi = \xi\omega / U_{conv}$ and $S_\eta = \eta\omega/U_c$ are the axial and circumferential Strouhal numbers, and a,b,c,d are constants to be

specified; U_{conv} and U_{ℓ} are, respectively, the convection and the centerline velocities. In equations (26) and (27) there should have been added the subscript Re for Reynolds number; but, at least in the range investigated by Bakewell, the effect of Reynolds number is small and does not appear explicitly in the expressions.

The values of the constants used in these two expressions for axial and circumferential correlations depend on the fluid. For turbulent flow in air, the values of a, b,c and d to be used in equations (26) and (27) with Strouhal numbers based on centreline velocity are given by [28]

$$a = 8.7266,\ b = 1.0,\ \text{for } S_{\xi} = \xi\omega / U_{\ell},$$
$$c = 20,\ d = 100,\ \text{for } S_{\eta} = \eta\omega / U_{\ell}. \qquad (28)$$

It may be expected, nevertheless, that these constants would be approximately the same for different fluids at the same Strouhal number, at least for sufficiently high Reynolds number. This was supported by Clinch's measurements in water [30], of which the authors have become aware after the completion of this part of the work.

Bakewell also obtained measurements of the mean square pressure per unit band-width, $\overline{p_{\omega}^2(t)}$, which are reproduced in Figure 4 plotted against Strouhal number $2r\omega/U_{\ell}$. For the purpose of this analysis, the following expression for the curve of best fit was obtained by the authors:

$$\overline{p_{\omega}^2\ (t)} = 2k_2\ \rho_F^2\ r\ U_{\ell}^3\ \ e^{-2k_1 r\omega/U_{\ell}}\ , \qquad (29)$$

where $k_1 = 0.25$ and $k_2 = 2 \times 10^{-6}$; ρ_F is the density of the fluid.

Upon substituting the experimentally based relations (26) - (29) into equations (25) and thence into equations (23) we obtain expressions for the cross-correlation spectral densities of the force field arising from boundary-layer pressure fluctuations. These expressions may then be substituted into equation (19) to obtain the following expression for the mean square response of the shell:

$$\overline{y_q^2(t)} = \sum_{n=1}^{4(N+1)-J} \Phi_{qn}^2 \frac{n^2}{16\pi^2\omega_n^4 M_n^2} \times$$

$$\times \left[\sum_{i=1}^{N+1}\sum_{\mu=1}^{N+1} \Phi_{in}\Phi_{\mu n} \left|\Gamma_{i\mu}^{F}\right| + 2\sum_{i=1}^{N+1}\sum_{k=1}^{N+1} \Phi_{in}\Phi_{kn}\left|\Gamma_{ki}^{M}\right| \right.$$

$$\left. + \sum_{j=1}^{N+1}\sum_{k=1}^{N+1} \Phi_{jn}\Phi_{kn}\left|\Gamma_{jk}^{MM}\right| + \sum_{p=1}^{N+1}\sum_{\nu=1}^{N+1} \Phi_{pn}\Phi_{\nu n}\left|\Gamma_{p\nu}^{F}\right| \right] , \qquad (30)$$

where

$$\Gamma_{i\mu}^{F} = \frac{1}{(B^2+A^2)^2}\left\{ (B^2-A^2)\left[F_3^{C}(\ell_i'',\ell_\mu'') - F_3^{C}(\ell_i',\ell_\mu'') - F_3^{C}(\ell_i'',\ell_\mu') + F_3^{C}(\ell_i',\ell_\mu')\right] \right.$$

$$\left. + 2.AB\left[-F_3^{S}(\ell_i'',\ell_\mu'') + F_3^{S}(\ell_i',\ell_\mu'') + F_3^{S}(\ell_i'',\ell_\mu') - F_3^{S}(\ell_i',\ell_\mu')\right]\right\} , \qquad (31)$$

$$\Gamma^{M}_{ki} = \frac{1}{(A^2+B^2)^3}\left\{(B^3-3A^2B)\left[F_4^c(\ell''_k,\ell''_i)-F_4^c(\ell'_k,\ell''_i)-F_4^c(\ell''_k,\ell'_i)+F_4^c(\ell'_k,\ell'_i)\right]\right.$$
$$\left.+(A^3-3AB^2)\left[F_4^s(\ell''_k,\ell''_i)-F_4^s(\ell'_k,\ell''_i)-F_4^s(\ell''_k,\ell'_i)+F_4^s(\ell'_k,\ell'_i)\right]\right\}$$
$$+\frac{1}{(A^2+B^2)^2}\left\{(B^2-A^2)(\ell''_k-\ell_k)\left[F_3^c(\ell''_k,\ell''_i)-F_3^c(\ell''_k,\ell'_i)\right]\right.$$
$$-(B^2-A^2)(\ell'_k-\ell_k)\left[F_3^c(\ell'_k,\ell''_i)-F_3^c(\ell'_k,\ell'_i)\right]$$
$$-2AB(\ell''_k-\ell_k)\left[F_3^s(\ell''_k,\ell''_i)-F_3^s(\ell''_k,\ell'_i)\right]$$
$$\left.+2AB(\ell'_k-\ell_k)\left[F_3^s(\ell'_k,\ell''_i)-F_3^s(\ell'_k,\ell'_i)\right]\right\}, \qquad (32)$$

$$\Gamma^{MM}_{jk} = \frac{1}{(A^2+B^2)^2}\left\{(B^2-A^2)(\ell_k-\ell''_k)\left[(\ell_j-\ell''_j)F_3^c(\ell''_k,\ell''_j)-(\ell_j-\ell'_j)F_3^c(\ell''_k,\ell'_j)\right]\right.$$
$$-(B^2-A^2)(\ell_k-\ell'_k)\left[(\ell_j-\ell''_j)F_3^c(\ell'_k,\ell''_j)-(\ell_j-\ell'_j)F_3^c(\ell'_k,\ell'_j)\right]$$
$$-2AB(\ell_k-\ell''_k)\left[(\ell_j-\ell''_j)F_3^s(\ell''_k,\ell''_j)-(\ell_j-\ell'_j)F_3^s(\ell''_k,\ell'_j)\right]$$
$$\left.+2AB(\ell_k-\ell'_k)\left[(\ell_j-\ell''_j)F_3^s(\ell'_k,\ell''_j)-(\ell_j-\ell'_j)F_3^s(\ell'_k,\ell'_j)\right]\right\}$$
$$+\frac{1}{(A^2+B^2)^3}\left\{(\ell_k+\ell_j-\ell''_j-\ell''_k)\left[B(3A^2-B^2)F_4^c(\ell''_k,\ell''_j)+A(3B^2-A^2)F_4^s(\ell''_k,\ell''_j)\right]\right.$$
$$-(\ell_k+\ell_j-\ell'_j-\ell''_k)\left[B(3A^2-B^2)F_4^c(\ell''_k,\ell'_j)+A(3B^2-A^2)F_4^s(\ell''_k,\ell'_j)\right]$$
$$-(\ell_k+\ell_j-\ell''_j-\ell'_k)\left[B(3A^2-B^2)F_4^c(\ell'_k,\ell''_j)+A(3B^2-A^2)F_4^s(\ell'_k,\ell''_j)\right]$$
$$\left.+(\ell_k+\ell_j-\ell'_j-\ell'_k)\left[B(3A^2-B^2)F_4^c(\ell'_k,\ell'_j)+A(3B^2-A^2)F_4^s(\ell'_k,\ell'_j)\right]\right\}$$
$$+\frac{1}{(A^2+B^2)^4}\left\{\left[(A^2-B^2)^2-4A^2B^2\right]\left[F_5^c(\ell''_k,\ell''_j)-F_5^c(\ell''_k,\ell'_j)-F_5^c(\ell'_k,\ell''_j)+F_5^c(\ell'_k,\ell'_j)\right]\right.$$
$$\left.+4AB(A^2-B^2)\left[F_5^s(\ell''_k,\ell''_j)-F_5^s(\ell''_k,\ell'_j)-F_5^s(\ell'_k,\ell''_j)+F_5^s(\ell'_k,\ell'_j)\right]\right\}; \qquad (33)$$

Γ^{F}_{pv} has the same form as Γ^{F}_{iu} ; in equations (31)-(33) the constants are given by

$A = a/U_\ell$, $B = b/U_\ell$, $C = cr^2/U_\ell^2$, $D = dr^2/U_\ell^2$, and the functions F_i^C and F_i^S , $i = 3, 4, 5$ are given by

$$F_3^C(\ell_i,\ell_m) = \frac{K_2}{C_2}\int_0^\infty \frac{e^{-[(K_1+B|\ell_i-\ell_m|)\omega + (C_1/\omega)]}\cos[A|\ell_i-\ell_m|\omega]}{\omega^3\left[(\omega/\omega_2)^4 + (4\zeta_2^2-2)(\omega/\omega_2)^2+1\right]}\,d\omega$$

$$+\frac{K_2}{D_2}\int_0^\infty \frac{e^{-[(K_1+B|\ell_i-\ell_m|)\omega + (D_1/\omega)]}\cos[A|\ell_i-\ell_m|\omega]}{\omega^3\left[(\omega/\omega_2)^4 + (4\zeta_2^2-2)(\omega/\omega_2)^2+1\right]}\,d\omega \equiv \int_0^\infty J(\omega)\,d\omega, \quad (34)$$

$$F_3^S(\ell_i,\ell_m) = \frac{K_2}{C_2}\int_0^\infty \frac{e^{-[(K_1+B|\ell_i-\ell_m|)\omega + (C_1/\omega)]}\sin[A|\ell_i-\ell_m|\omega]}{\omega^3\left[(\omega/\omega_2)^4 + (4\zeta_2^2-2)(\omega/\omega_2)^2+1\right]}\,d\omega,$$

$$+\frac{K_2}{D_2}\int_0^\infty \frac{e^{-[(K_1+B|\ell_i-\ell_m|)\omega + (D_1/\omega)]}\sin[A|\ell_i-\ell_m|\omega]}{\omega^3\left[(\omega/\omega_2)^4 + (4\zeta_2^2-2)(\omega/\omega_2)^2+1\right]}\,d\omega \equiv \int_0^\infty Q(\omega)\,d\omega, \quad (35)$$

$$F_4^C(\ell_i,\ell_m) = \int_0^\infty [J(\omega)/\omega]\,d\omega, \quad (36)$$

$$F_4^S(\ell_i,\ell_m) = \int_0^\infty [Q(\omega)/\omega]\,d\omega, \quad (37)$$

$$F_5^C(\ell_i,\ell_m) = \int_0^\infty [J(\omega)/\omega^2]\,d\omega, \quad (38)$$

$$F_5^S(\ell_i,\ell_m) = \int_0^\infty [Q(\omega)/\omega^2]\,d\omega, \quad (39)$$

where $K_1 = 2k_1 r / U_\xi$, $K_2 = 2k_2 \rho_F^2 r U_\xi^3$,

$$C_1 = 1 / \sqrt{C},\ C_2 = \sqrt{C}\ (2 - e^{D/C}),$$
$$D_1 = \sqrt{(\ell n 2)/D},\quad D_2 = 2\sqrt{D(\ell n 2)}\ [1 - \tfrac{C}{D}\ \ell n\ 2]. \tag{40}$$

After integrating over ω, the functions F_i^c and F_i^s of equations (34) - (39) may be written as follows:

$$F_3^c(\ell_i,\ell_w) = \frac{\pi K_2}{8 C_2 \omega_n^2}\left[4e^{-\gamma_1}\sin\gamma_2 - 4e^{-\gamma_3}\sin\gamma_4 + \frac{1}{\zeta_n}\left(e^{-\gamma_1}\cos\gamma_2 + e^{-\gamma_3}\cos\gamma_4\right)\right]$$
$$+ \frac{\pi K_2}{8 D_2 \omega_n^2}\left[4e^{-\gamma_5}\sin\gamma_6 - 4e^{-\gamma_7}\sin\gamma_8 + \frac{1}{\zeta_n}\left(e^{-\gamma_5}\cos\gamma_6 + e^{-\gamma_7}\cos\gamma_8\right)\right], \tag{41}$$

$$F_3^s(\ell_i,\ell_w) = \frac{\pi K_2}{8 C_2 \omega_n^2}\left[4e^{-\gamma_3}\cos\gamma_4 - 4e^{-\gamma_1}\cos\gamma_2 + \frac{1}{\zeta_n}\left(e^{-\gamma_1}\sin\gamma_2 + e^{-\gamma_3}\sin\gamma_4\right)\right]$$
$$+ \frac{\pi K_2}{8 D_2 \omega_n^2}\left[4e^{-\gamma_7}\cos\gamma_8 - 4e^{-\gamma_5}\cos\gamma_6 + \frac{1}{\zeta_n}\left(e^{-\gamma_5}\sin\gamma_6 + e^{-\gamma_7}\sin\gamma_8\right)\right], \tag{42}$$

$$F_4^c(\ell_i,\ell_w) = \frac{\pi K_2}{8 C_2 \omega_n^3}\left[e^{-\gamma_1}\sin\gamma_2 - e^{-\gamma_3}\sin\gamma_4\right] + \frac{\pi K_2}{8 D_2 \omega_n^3}\left[e^{-\gamma_5}\sin\gamma_6 - e^{-\gamma_7}\sin\gamma_8\right]$$
$$+ \frac{1}{\omega_n} F_3^c(\ell_i,\ell_w), \tag{43}$$

$$F_4^s(\ell_i,\ell_w) = \frac{\pi K_2}{8 C_2 \omega_n^3}\left[e^{-\gamma_3}\cos\gamma_4 - e^{-\gamma_1}\cos\gamma_2\right] + \frac{\pi K_2}{8 D_2 \omega_n^3}\left[e^{-\gamma_7}\cos\gamma_8 - e^{-\gamma_5}\cos\gamma_6\right]$$
$$+ \frac{1}{\omega_n} F_3^s(\ell_i,\ell_w), \tag{44}$$

$$F_5^c(\ell_i,\ell_w) = \frac{2}{\omega_n} F_4^c - \frac{1}{\omega_n^2} F_3^c, \tag{45}$$

$$F_5^s(\ell_i,\ell_u) = \frac{2}{\omega_2} F_4^s - \frac{1}{\omega^2} F_3^s \,, \tag{46}$$

where

$$\gamma_1^* = \left[K_1 + |\ell_i - \ell_u|\,(A\zeta_n + B)\right]\omega_n + \frac{C_1}{\omega_n(1+\zeta_n^2)} \,,$$

$$\gamma_2 = \left[-K_1\zeta_n + |\ell_i - \ell_u|\,(A - B\zeta_n)\right]\omega_n + \frac{C_1\varphi_n}{\omega_n(1+\zeta_n^2)} \,,$$

$$\gamma_3 = \left[+K_1 - |\ell_i - \ell_u|\,(A\zeta_n - B)\right]\omega_n + \frac{C_1}{\omega_n(1+\zeta_n^2)} \,,$$

$$\gamma_4 = \left[+K_1\zeta_n + |\ell_i - \ell_u|\,(A + B\zeta_n)\right]\omega_n - \frac{C_1\zeta_n}{\omega_n(1+\zeta_n^2)} \,,$$

$$\gamma_5 = \left[K_1 + |\ell_i - \ell_u|\,(A\zeta_n + B)\right]\omega_n + \frac{D_1}{\omega_n(1+\zeta_n^2)} \,, \tag{47}$$

$$\gamma_6 = \left[-K_1\zeta_n + |\ell_i - \ell_u|\,(A - B\zeta_n)\right]\omega_n + \frac{D_1\zeta_n}{\omega_n(1+\zeta_n^2)} \,,$$

$$\gamma_7 = \left[+K_1 - |\ell_i - \ell_u|\,(A\zeta_n - B)\right]\omega_n + \frac{D_1}{\omega_n(1+\zeta_n^2)} \,,$$

$$\gamma_8 = \left[+K_1\zeta_n + |\ell_i - \ell_u|\,(A + B\zeta_n)\right]\omega_n - \frac{D_1\zeta_n}{\omega_n(1+\zeta_n^2)} \,.$$

Here the arguments (ℓ_i, ℓ_u) have been omitted from $\gamma_1(\ell_i, \ell_u)$ $\gamma_2(\ell_i, \ell_u)$, etc., for simplicity.

The response of the shell to a subsonic boundary-layer pressure field is given by equation (30) with the Γ's given by equations (31) - (33) and the other terms involved given by equations (40) - (47).

5. CALCULATIONS AND DISCUSSION

To determine the response of a cylindrical shell to a random pressure field we must proceed as follows:

(a) The shell must be subdivided into a sufficient number of finite elements (sufficiency in this context will be discussed later).

(b) For a given value of n, the mass and stiffness matrices for each finite element must be determined.

(c) The global mass and stiffness matrices must be constructed.

(d) The eigenvalues and eigenvectors must be computed.

(e) The r.m.s. response must be computed at each node.

The necessary steps of the computational method for determining the eigenvalues and eigenvectors have been outlined in reference [13]. The additional computational task, for determining the r.m.s. response, is evident from the work presented here. In the case of an arbitrary but specified pressure field we must proceed through equation (19); in the case of a boundary-layer pressure field, on the other hand, we must proceed with equation (30) et seq., where a great deal of the computational task has already been carried out.

A computer program has been written for carrying out steps (a) - (e) of the calculation and determining the response in the case of boundary-layer pressure fields. It is written in Fortran IV language for the IBM 360/75 computer,

using double precision arithmetic throughout the eight overlays shown in Figure 5.

The necessary time for the calculation of r.m.s. response for a typical case involving five finite elements is approximately 20 mins. This computer time seems to be high. The time quoted above refers to the case where all the computed natural frequencies are used in the calculation of response. However, if only a few of the lowest natural frequencies are used in the calculation, the response may be computed to an acceptable degree of accuracy, but with considerable saving in computational cost; thus, if only 15% of the natural frequencies are utilized, then the time given above may be reduced by a factor of 1/8 approximately. Moreover, the computer calculation involves the determination of $(\overline{u_n^2})^{1/2}$, $(\overline{v_n^2})^{1/2}$, $(\overline{w_n^2})^{1/2}$, and $[\overline{(dw_n/dx)^2}]^{1/2}$ at every nodal point. Accordingly, large savings in time may be realized if the response is not required at every node, or if only the r.m.s. radial displacement is desired.

As developed previously, the present theory, and the computer program based upon it, is capable of determining the r.m.s. response of the general case of an axially non-uniform, thin cylindrical shell, subjected to subsonic boundary layer pressure fluctuations, with arbitrary boundary conditions.

Some calculations were conducted to illustrate the theory. The first set of calculations was for a simply-supported uniform shell with the following dimensions and material properties:

$r = 4.08$ in., $t = 0.047$ in., $L = 18.54$ in., $E = 3 \times 10^7$ lb./in.^{2}, $\nu = 0.3$ and $\rho = 7.324 \times 10^{-4}$ lb.-sec.^{2}/in.^{4}. The fluid is air at 70°F and atmospheric pressure, flowing through the shell. The density of the air is taken as $\rho_F = 0.2329 \times 10^{-2}$ lb.sec.^{2}/ft.^{4} and its kinematic viscosity $\nu_F = 1.631 \times 10^{-4}$ ft.^{2}/sec.

The free vibration characteristics of this particular shell in vacuo was studied in reference [13]. From Figure 6, it is clear that an idealization of the continuous structure by five finite elements is sufficient to yield reasonably accurate results for low as well as high natural frequencies.

The first case studied was for mean centreline velocity of 24 ft./sec. corresponding to $Re = 10^5$ and a damping factor of $\zeta_r = 10^{-5}$. The results of maximum r.m.s. response for n = 2,3,4 and 5 are shown in Figure 7. We note that peak values for $(\sqrt{\overline{v_n^2}})_{max}$, $(\sqrt{\overline{u_n^2}})_{max}$ and $(\sqrt{\overline{w_n^2}})_{max}$ are at n = 3. This confirms the theoretical result, as obtained in equation (30), that the r.m.s. response is inversely proportional to the square of the natural frequency, ω_r; the minimum natural frequencies in this case correspond to n = 3 (Figures 6 and 7).

If the total response is desired, as would be the case in most applications, this may be obtained by summation over n [see equation (2)].

In this particular case, the circumferential mode of greatest interest is n = 3, as it is in this mode that

the highest response is obtained. Consequently all subsequent calculations are confined to this particular value of n.

Figure 8 shows the r.m.s. response for different mean velocities, namely 24, 75, 120 and 240 ft./sec., using $\zeta_r = 10^{-5}$ and 10^{-2} as damping factors. It is seen, from the results plotted in Figure 8, that the r.m.s. displacement is inversely proportional to the damping factor and proportional to the mean axial flow velocity raised to the power 2.2, approximately, both effects being as could have been anticipated.

The second set of calculations undertaken was for a shell first studied by Clinch, both theoretically and experimentally [9]. It is a very long, slender and thin cylindrical shell ($r = 3$ in., $L = 240$ in., $t = 0.025$ in., $E = 28.5 \times 10^6$ lb/in.^{2}, $\nu = 0.305$, $\rho = 0.749 \times 10^{-3}$ lb.sec^2/in.^{4}) conveying water with flow velocities in the range 248 - 520 in/sec. Clinch obtained experimental data of the mean square radial displacement of the shell in frequency bands corresponding to the third-octave filters he used. Then, by summation, he obtained the response in the frequency range of 100 - 1,000 Hz approximately; the response in only this frequency range is given in reference [9] where it is compared with Clinch's own theory which, as was discussed in the Introduction, only deals with the high-frequency response of cylindrical shells. Moreover, the experimental values of the mean square radial dis-

placements given by Clinch are mean values of measurements taken at several locations on the shell.

This shell was analysed by our theory by subdividing the shell into 8 identical finite elements; the boundary conditions were taken to be those of simple support. The natural frequencies of the shell were calculated first, and it was found that many of the natural frequencies of the shell for $n = 2$ and $n = 3$ were below 100 Hz, indicating that the high-frequency response as calculated and measured by Clinch would likely differ appreciably from the total response.

Calculations of the response were confined to $n = 2$ to 6 (from which the approximate 'total' response was obtained by summation), and to the lowest and highest flow velocities used by Clinch. The values of this 'total' response of the shell at its axial mid-point are shown in Figure 9. Also shown in Figure 9 are values of the high-frequency response, as calculated by this theory, obtained by taking into account only the modes whose natural frequencies are in the range 93 - 1,000 Hz; also shown are Clinch's experimental results.

It is immediately evident from Figure 9 that the response at the high frequency range is but a small part of the total. Thus, at the flow velocity of 248 in/sec the total mean square response is 3.2×10^{-8} in.^{2} whereas the high-frequency response is 8×10^{-11} in.^{2}, approximately, giving a ratio of 20:1 for the corresponding r.m.s. values; the difference at

higher flow velocities is even more pronounced. This is not a criticism of Clinch's work, but it does demonstrate the limitations of his theory if one is interested in the total response of the shell, rather than only the high-frequency response. It should be added that for shorter shells than this one the discrepancy between total and high-frequency response values would be less pronounced.

The second point of interest in Figure 9 is that agreement between this theory and experiment, in the frequency range of 100 - 1,000 Hz approximately, is quite good. This is the first and, so far, only experimental verification of this theory, as experimental data are very scarce; the results lend confidence that the values of the overall response of the shell may also be reliable. In this connection, regarding agreement between theory and experiment, the following points should be made:

(a) In the experiments, the ends of the shell were probably more nearly clamped than simply supported; this would tend to lower the theoretical values slightly, although for such a long shell, this effect must be quite small.

(b) The experimental values given by Clinch are 'mean' values taken at a number of locations; hence, they must be lower than the theoretical values which are associated with the location of maximum response.

(c) The calculations were carried out with $\zeta_r = 2 \times 10^{-2}$,

for all r, as given by Clinch, although as he points out this value was obtained experimentally by actually exciting the shell in what may have been one of its beam modes. The experimental difficulties in this connection are well appreciated by the authors; nevertheless, the simplification of using a single damping coefficient is doubtlessly only approximately correct, at best.

(d) In the theory, the response was calculated by summing the results of calculations with n = 2 to n = 6 only (to limit the computational cost). Whereas most of the contribution to the 'total' response was associated with n = 2 and n = 3 (Table 1), and whereas the contribution of n = 5 and n = 6 is already small, amounting to less than 1.5% of this 'total', it should be recognized that the values given here are only approximate; if the total response were calculated using a much higher number of circumferential wavenumbers, the response obtained would be higher, although almost certainly no more than 2% higher.

(e) The contribution to the total response diminishes very drastically with increasing frequency; accordingly, the high-frequency response calculated for the frequency range of 93 - 1,000 Hz is appreciably higher than for 100 - 1,000 Hz, let us say.

(f) Clinch's own theoretical values of the response (only given as functions of frequency; Fig. 13 of [9]), are

	U_ℓ = 248 in/sec			U_ℓ = 520 in/sec		
n	$(\overline{u_n^2})^{1/2}$	$(\overline{v_n^2})^{1/2}$	$(\overline{w_n^2})^{1/2}$	$(\overline{u_n^2})^{1/2}$	$(\overline{v_n^2})^{1/2}$	$(\overline{w_n^2})^{1/2}$
2	3.6×10^{-6}	9.0×10^{-5}	1.8×10^{-4}	2.8×10^{-5}	6.7×10^{-4}	1.3×10^{-3}
3	3.3×10^{-7}	3.3×10^{-6}	9.8×10^{-6}	3.9×10^{-6}	3.4×10^{-5}	1.0×10^{-4}
4	1.8×10^{-7}	4.2×10^{-7}	1.7×10^{-6}	3.0×10^{-6}	5.3×10^{-6}	2.1×10^{-5}
5	2.0×10^{-8}	7.3×10^{-8}	3.6×10^{-7}	5.7×10^{-7}	1.2×10^{-6}	5.9×10^{-6}
6	4.3×10^{-9}	7.3×10^{-8}	5.2×10^{-7}	2.5×10^{-7}	1.9×10^{-6}	1.2×10^{-5}

TABLE 1. Variation of the r.m.s. response with n.

higher than his experimental values at the high flow velocity.

The results obtained by this theory (Figure 9) indicate that the total r.m.s. radial-displacement response is proportional to flow velocity raised to the 2.7 power, approximately.

Some further results obtained in the course of this particular set of calculations are presented in Figures 10 - 12. Figure 10 shows the mean square response of the shell at its mid-point, not only in terms of the radial displacement, but also of the axial and circumferential displacements.

In Figure 11 we see the components of the response at each of the natural frequencies of the system, for n = 2 and a flow velocity of 248 in/sec; Figure 11 shows the corresponding results for U_ℓ = 520 in/sec. Here we see clearly that the

largest contributions to the response of this shell are at frequencies below 100 Hz. We also note that the contributions of the even axial modes are zero; this is as it should be, because of symmetry. The results for other values of n are quite similar.

6. CONCLUSION

In this paper we have presented a theory capable of predicting the response, to an arbitrary random pressure field, of an axially symmetric, non-uniform, thin cylindrical shell. To this end the shell is subdivided into a number of cylindrical finite elements, each with two nodes, the nodal displacements being the axial, circumferential and radial displacements and a rotation. The pressure field is similarly rendered discrete and is represented by two forces and a moment at each node. The analysis proceeds separately for each circumferential wavenumber, n, and the response is given in terms of r.m.s. values of the nodal displacements; the total response may then be found by summing over n.

A special form of the theory was developed for the case where the pressure field arises from pressure fluctuations in the turbulent boundary layer of an internally flowing fluid. This theory was computerized so that if the dimensions and material properties of each finite element,and the properties and flow velocity of the fluid, are given as inputs, the program gives as output the natural frequencies and eigenvectors of the shell and the r.m.s. values of the nodal displacements.

A number of assumptions and simplifications were introduced into the theory either for expediency or lest excessive generality render it unwieldy. A compendium of the most important ones is given here.

(i) The shell is assumed to be thin and geometrically axially symmetric, although it may be axially non-uniform.

(ii) It is implicitly presumed that a sufficient number of finite elements is utilized in each case, so that no significant loss of detail is suffered in transforming the continuous system to a discrete one. (In this theory, 5 to 10 finite elements should be sufficient to adequately analyse most shells.)

(iii) The damping (damping matrix) is assumed to be such that decoupling of the equations of motion may be effected.

(iv) The pressure field is assumed to be stationary, ergodic and homogeneous.

(v) In calculating the response it is assumed that there is no coupling between the circumferential wavenumbers.

(vi) The contribution of cross-product terms to the mean square response is assumed to be negligible (equations 16 to 17).

Where the pressure field arises from internal flow, the following additional assumptions were made in the special form of the theory developed for this case:

(vii) the only source of excitation arises from pressure fluctuations in the turbulent boundary layer;

(viii) non-inertial dynamical effects of the mean flow are small (§4.1) in most applications of practical interest and may be neglected;

(ix) the frictional losses in the length of the shell are small and may be neglected;

(x) pressurization and compressibility effects are negligible;

(xi) Bakewell's correlation functions for the pressure field are applicable to any fluid, provided that the Reynolds number is not too small.

These assumptions, when grouped as above, may appear to render the theory insufficiently general. On closer examination, however, this theory is found to be applicable to a large number of physical problems of practical interest; moreover, some of these assumptions may be eliminated by simple extensions of the theory, should a physical problem present itself warranting the effort [e.g. (ix) and (x) above]. To the authors' knowledge, this is the most general theory presently available for the physical problem at hand. In this connection, it should be noted that this theory is equally applicable to cases where the shell is subjected to an external, rather than internal, pressure field, including the case where the pressure field arises from an external axial flow.

7. ACKNOWLEDGEMENTS

This research was supported by the National Research Council of Canada (Grant No. A4366) whose assistance is hereby gratefully acknowledged. The authors also acknowledge the assistance rendered by the McGill Computing Centre in bearing part of the cost incurred in the computational task.

APPENDIX

Notation

a,b,c,d - constants defined by equation (28)

A,B,C,D - parameters defined in equation (33)

C_1,C_2,D_1,D_2 - parameters defined in equation (40)

$f_R(x,t)$, $f_C(x,t)$ - instantaneous radial and circumferential forces per unit length

$\overline{f_\Omega f_\Omega'}$ - mean of the force f per unit bandwidth

$F_3^C(\ell_i,\ell_u)$, F_3^S, F_4^C, F_4^S, F_5^C, F_5^S - parameters defined in equations (34) - (39)

$|H_r(\Omega)|$ - magnification factor defined by (16)

J - number of constraints imposed

k_1, k_2 - constants defined by equation (29)

K_1, K_2 - parameters defined by equation (40)

ℓ - length of finite element

ℓ_e - coordinate of node e in the x-direction

ℓ_e', ℓ_e'' - coordinates of the area S_e, surrounding the node e, with respect to the origin in the x-direction (Fig. 2)

L - total length of shell

m - axial half wavenumber

$\mathfrak{M}_r$ - moment acting at a node as shown in Figure 2b

M_r - rth element of the (diagonal) generalized mass matrix

n	- circumferential wavenumber
N	- number of finite elements in the structure
$p(x,\phi,t)$	- instantaneous pressure on the surface
$\overline{p^2(x,\phi,t)}$	- mean square of pressure fluctuations
$\overline{p_\Omega^2(t)}$	- mean square pressure per unit bandwidth of a homogeneous pressure field
r	- mean radius of shell
S_ξ, S_η	- axial and circumferential Strouhal number, respectively
S_e	- area surrounding the node e (Fig. 2)
$F_j(\Omega)$	- Fourier transform of $f_j(t)$
$F_j^*(\Omega)$	- complex conjugate of $F_j(\Omega)$
t	- wall-thickness of shell, or time.
T	- half-period
U,V,W	- axial, circumferential and radial displacement
U_ℓ, U_{CONV}	- centerline and convection velocities, respectively
$\bar{U}$	- mean flow velocity
u_n, v_n, w_n	- amplitudes of U,V,W associated with nth circumferential wavenumber
$W_f(x_i,x_j;\Omega,0)$	- cross-correlation spectral density function of the force field f
x	- axial coordinate

$\overline{y_q^2(x_g,\phi,t)}$ - mean square displacement of u_n, v_n, w_n or dw_n/dx at node for which $x = x_g$.

$z(t)$ - normal coordinate at time t

Γ^F_{iu}, Γ^M_{ki}, Γ^{MM}_{jk} - expressions defined in equations (31) - (33)

$\gamma_1(\ell_i,\ell_u)$, γ_2, . . . γ_8 - expressions defined in equation (47)

ζ_r - generalized damping factor

η - equal to $|r(\phi_i - \phi_j)|$

θ_r - phase lag of the displacement relative to the driving force; defined by equation (16)

ν - Poisson's ratio

ξ - equal to $|x_i - x_j|$

ρ - density of material of the shell

ρ_F - fluid density

τ - time delay

ϕ - circumferential coordinate

$\psi_{y_{ij}}(x_k,x_\ell;\ \phi_o,\tau)$ - spatial correlation function of the displacement defined by equation (13)

$\psi_p(\xi,\eta,\tau)$ - normalized space-time correlation function of the fluctuating pressure of a homogeneous field

$\psi_{p_\Omega}(\xi,\ 0,\ 0)$, $\psi_{p_\Omega}(0,\ \eta,\ 0)$ - axial and circumferential correlation functions of the fluctuating pressure per unit band-width with centre frequency Ω

ω - excitation frequency in Hz

ω_i - ith natural frequency in Hz

Ω - excitation circular frequency (rad/sec.)

Ω_i - ith natural circular frequency (rad/sec.)

$F(x,\phi,t)$ - vector of external forces

$\underset{\sim}{k}$ - stiffness matrix for one finite element

$\underset{\sim}{K}$ - stiffness matrix for the whole shell

$\underset{\sim}{m}$ - mass matrix for one finite element

$\underset{\sim}{M}$ - mass matrix for the whole shell

$\underset{\sim}{M}$ - generalized mass matrix (for the whole shell)

$\underset{\sim}{S}$ - spectral matrix (for the whole shell)

$\underset{\sim}{y}$ - displacement vector defined by equation (1)

$\underset{\sim}{z}(t)$ - normal coordinates vector

$\underset{\sim}{\delta}_i$, $\underset{\sim}{\delta}_j$ - nodal displacement vectors, at nodes i and j, respectively

$\underset{\sim}{\Phi}$ - modal matrix of the system

$\underset{\sim}{\Phi}_r$ - rth eigenvector of the system

REFERENCES

1. I. DYER 1959 The Journal of the Acoustical Society of America 31, 922-928. Response of plates to a decaying and convecting random pressure field.
2. A.C. ERINGEN 1957 Journal of Applied Mechanics 24, 46 - 53. Response of beams and plates to random loads.
3. D.H. TACK and R.F. LAMBERT 1962 Journal of the Aerospace Sciences 29, 311-322. Response of bars and plates to boundary-layer turbulence.
4. C.A. MERCER 1965 Journal of Sound and Vibration 2, 293-306. Response of a multi-supported beam to a random pressure field.
5. J.R. REAVIS 1967 Transactions of the American Nuclear Society 10, 369-370. WVI-Westinghouse vibration correlation for maximum fuel element displacement in parallel turbulent flow.
6. S.S. CHEN and M.W. WAMBSGANSS 1970 Argonne National Laboratory Report ANL-7685. Proceedings of the Conference on Flow-Induced Vibrations in Reactor System Components, pp. 5-31. Response of a flexible rod to near-field flow noise.
7. R.M. KANAZAWA and A.P. BORESI 1970 Argonne National Laboratory Report ANL-7685, pp. 47-63. Calcualtion of the response of rods to boundary layer pressure fluctuations.

8. M.G. COTTIS and J.G. JASONIDES 1964 Acoustical Fatigue in Aerospace Structures: Proceedings of the Second International Conference. Conference sponsored by U.S.A.F. Materials Laboratory, Dayton, Ohio, U.S.A. 29th April - 1st May. The response of a finite thin cylindrical shell to random pressure fields.

9. J.M. CLINCH 1970 Journal of Sound and Vibration 12, 429-451. Prediction and measurement of the vibrations induced in thin-walled pipes by the passage of internal turbulent water flow.

10. M.G. COTTIS 1968 Journal of Sound and Vibration 7, 31-38. On the dynamic response of an orthotropic finite shell to an arbitrary pressure field.

11. A. POWELL 1958 The Journal of the Acoustical Society of America 30, 1130-1135. Vibrations excited by random pressure fields.

12. A.A. LAKIS and M.P. PAÏDOUSSIS 1970 Mechanical Engineering Research Laboratories Report 70-9, McGill University. Dynamical analysis of axially non-uniform, thin cylindrical shells. I. Matrix formulation.

13. A.A. LAKIS and M.P. PAÏDOUSSIS 1972 Journal of Mechanical Engineering Science 14, 49 - 71. Dynamic analysis of axially non-uniform thin cylindrical shells.

14. A.A. LAKIS 1971 Ph.D. Thesis, McGill University. Free vibration and response to random pressure field of non-uniform cylindrical shells.

15. H.P. BAKEWELL Jr., G.F. CAREY, J.J. LIBUHA, H.H. SCHLOEMER and W.A. VON WINKLE 1962 U.S. Navy Underwater Sound Lab. Report No. 559. Wall pressure fluctuations in turbulent pipe flow.

16. J.L. SANDERS 1959 NASA TR-R24. An improved first approximation theory for thin shells.

17. B. BUDIANSKY and J.L. SANDERS 1963 Progress in Applied Mechanics, the Prager Anniversary Volume, pp. 129-140. On the "best" first order linear shell theory.

18. O.C. ZIENKIEWICZ and Y.K. CHEUNG 1968 The Finite Element Method in Structural and Continuum Mechanics. New York: McGraw-Hill.

19. A.A. LAKIS and M.P. PAIDOUSSIS 1971 Journal of Sound and Vibration 19, 1-15. Free vibration of cylindrical

tubular cantilevers conveying fluid. I. Theory.

24. M.W. SMITH and R.F. LAMBERT 1960 The Journal of the Acoustical Society of America 32, 512 - 514. Propagation of band limited noise.

25. W.W. WILLMARTH 1958 NACA TN-4139. Wall pressure fluctuations in a turbulent boundary layer.

26. P.F.R. WEYERS 1960 NASA TN-D-430. Vibration and near-field sound of thin-walled cylinders caused by internal turbulent flow.

27. G.M. CORCOS and H.W. LIEPMANN 1956 NACA TM-1420. On the contribution of turbulent boundary layers to the noise inside a fuselage.

28. H.P. BAKEWELL Jr. 1964 The Journal of the Acoustical Society of America 36, 146-148. Narrow-band investigations of the longitudinal space-time correlation function in turbulent airflow.

29. W.W. WILLMARTH and F.W. ROOS 1965 Journal of Fluid Mechanics 22, 81 - 95. Resolution and structure of the wall pressure field beneath a turbulent boundary layer.

30. J.M. CLINCH 1969 Journal of Sound and Vibration 9, 398 - 420. Measurements of the wall pressure field at the surface of a smooth-walled pipe containing turbulent water flow.

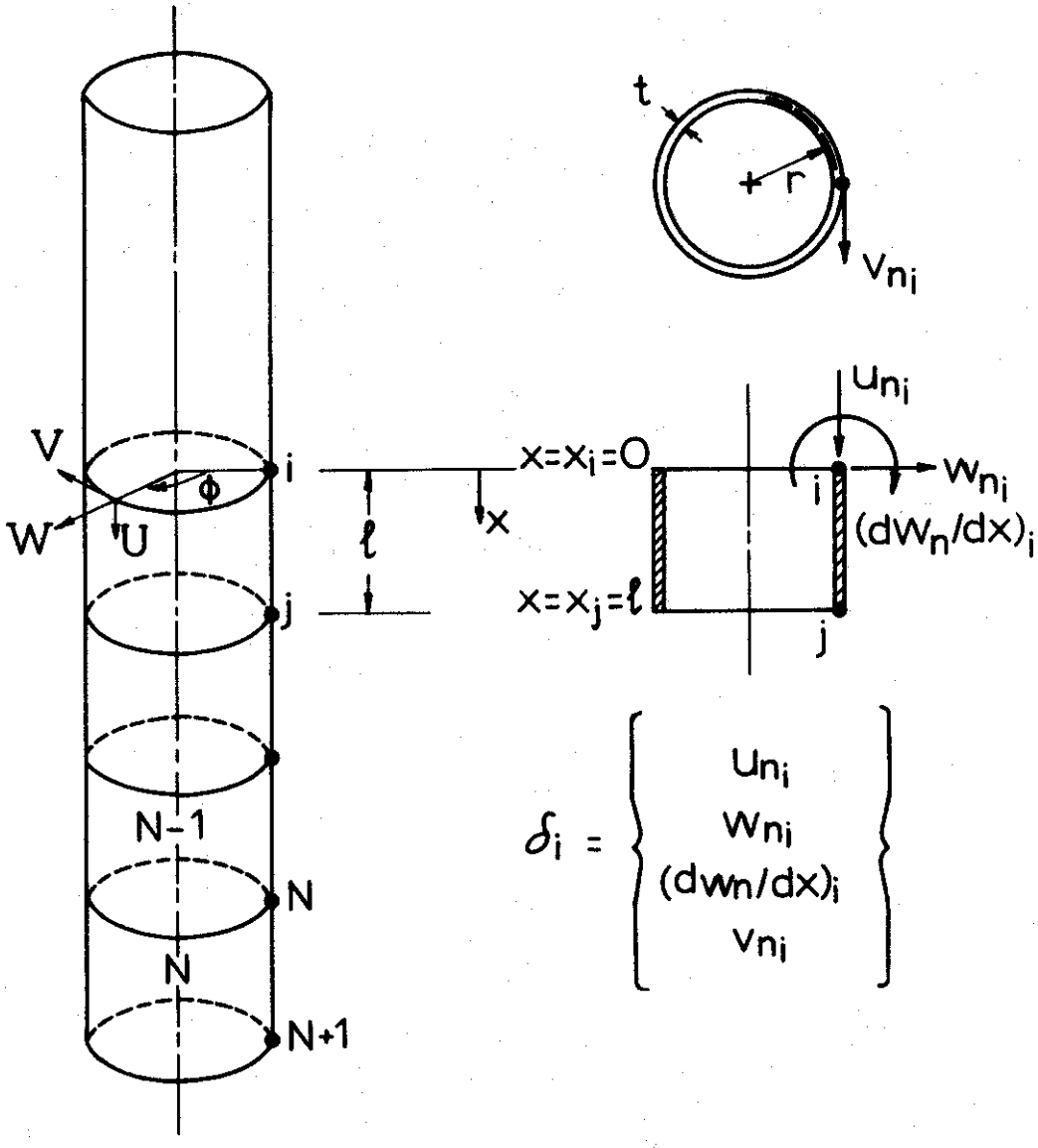

FIGURE 1 Definitions of the finite element used and of the displacement vector $\underset{\sim}{\delta}_i$.

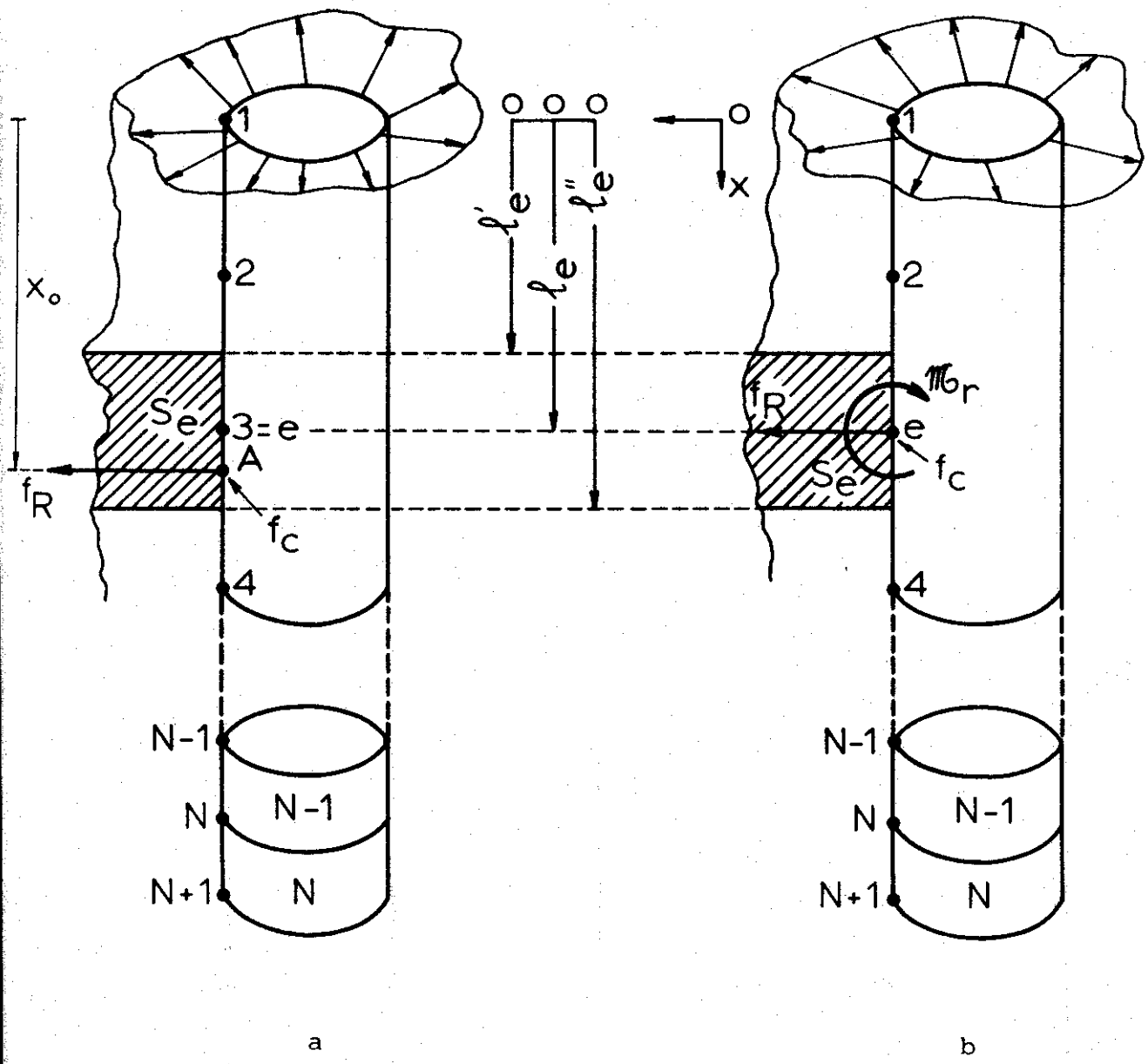

FIGURE 2 (a) Transformation of the continuous pressure field to a discrete force field

(b) The equivalent discrete force field acting at the node, e, involving f_R, f_C and m_r.

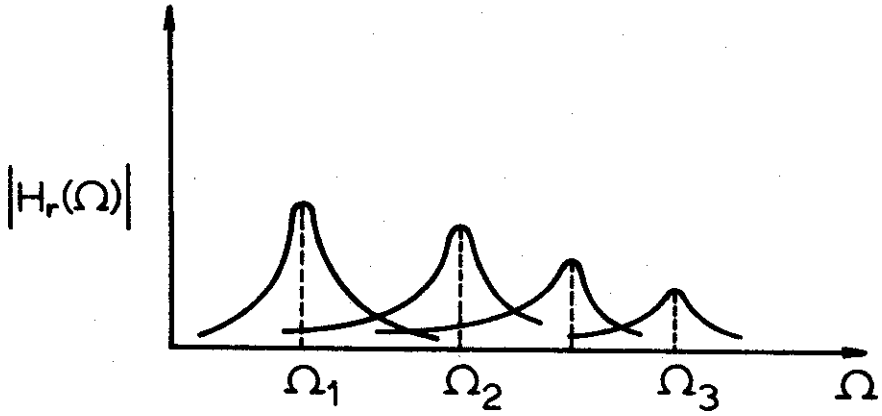

FIGURE 3 The magnification factor as a function of frequency for several modes

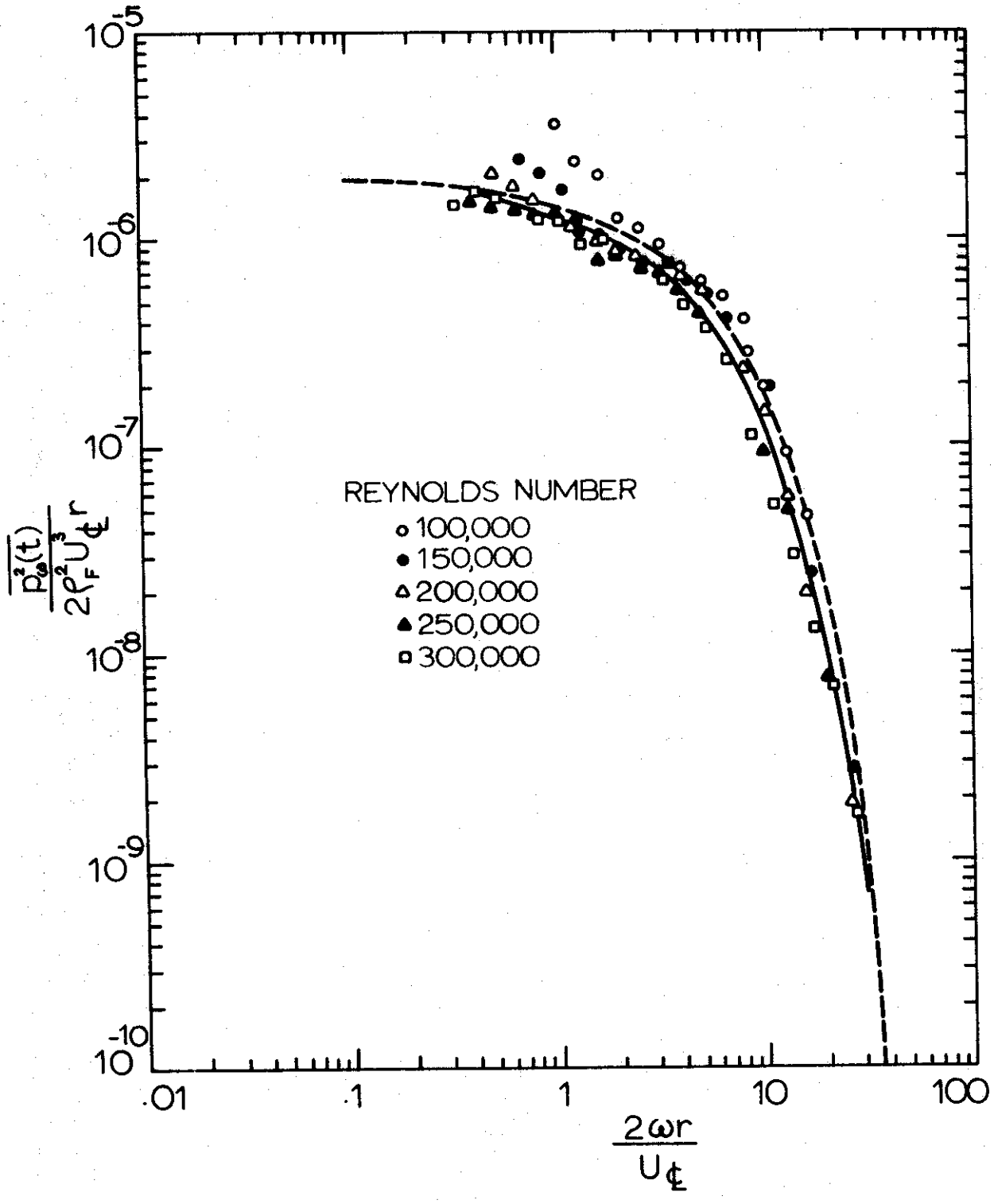

FIGURE 4 Bakewell's measurements of the mean square pressure per unit band-width, compared with the expression used in this theory. _____ Bakewell's line of best fit; _ _ _ _ equation (29) of this paper.

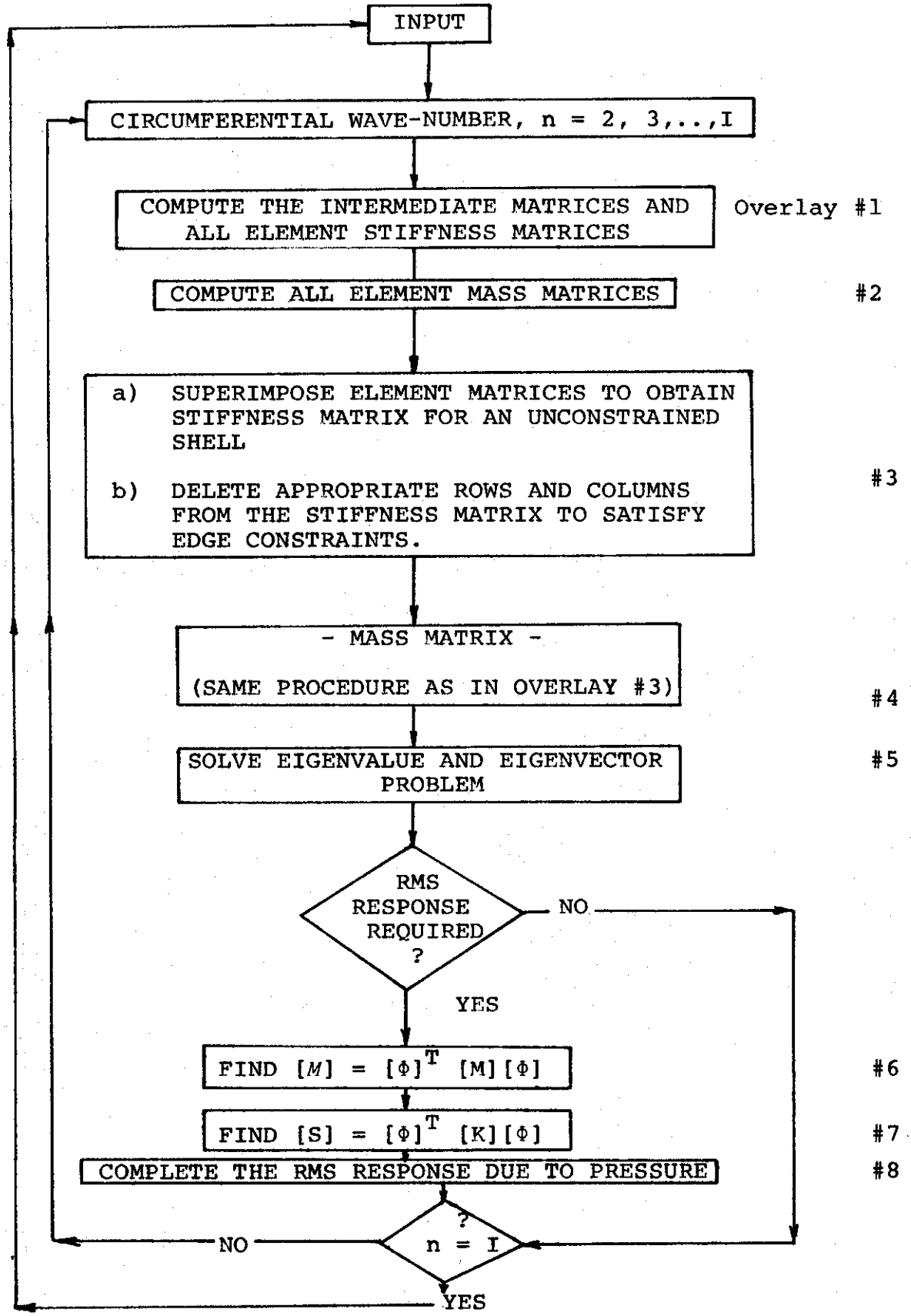

FIGURE 5. Computational flow diagram.

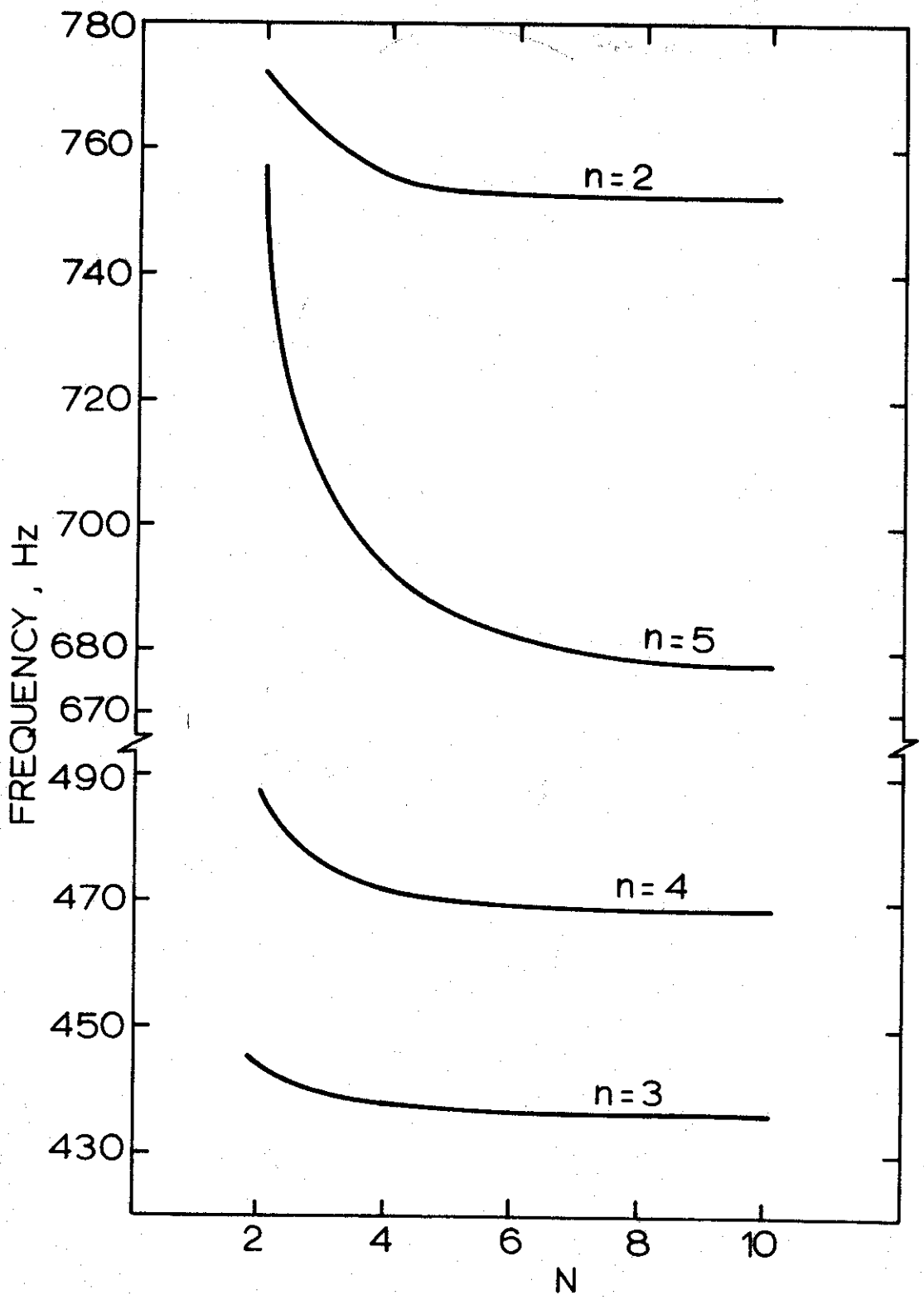

FIGURE 6 The natural frequencies of a simply-supported shell as functions of the number of finite elements used, N, for m = 1. (Continuous lines drawn through discrete points.)

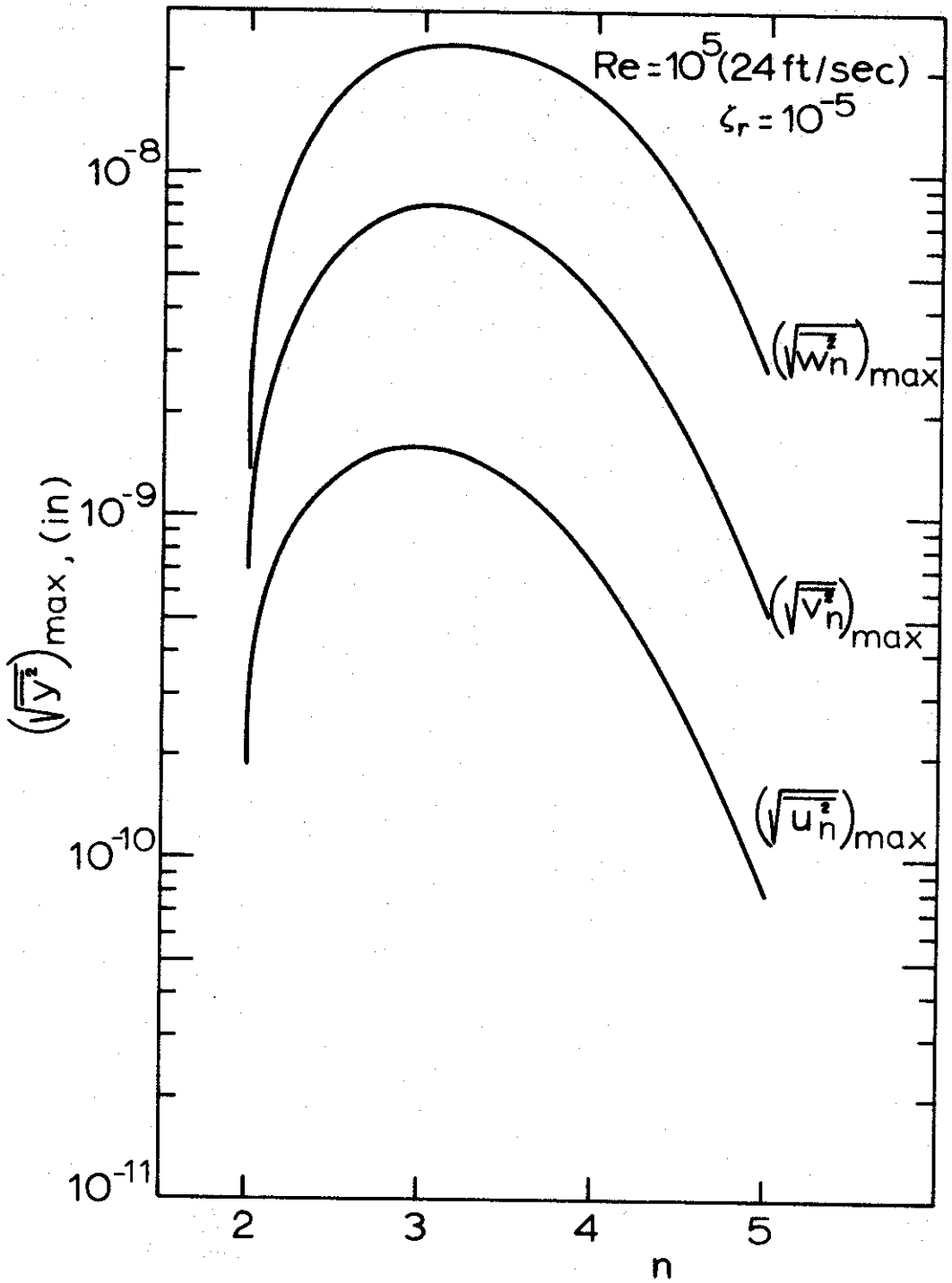

IGURE 7 Maximum r.m.s. displacements of a simply-supported shell (r = 4.08 in., t = 0.047 in., L = 18.54 in., steel shell conveying air) as functions of n; Re = 10^5 and $\zeta_r = 10^{-5}$.

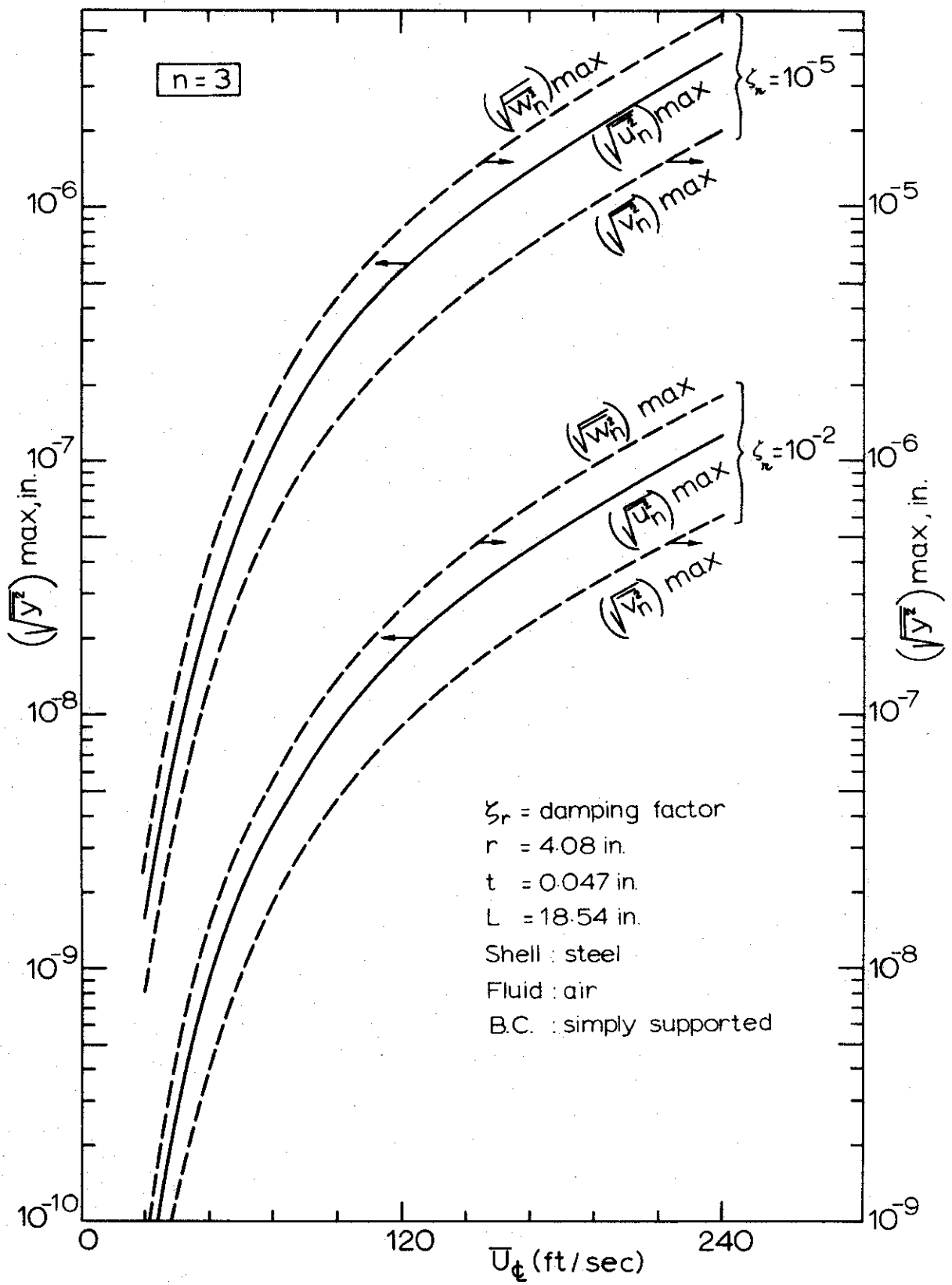

FIGURE 8 Maximum r.m.s. displacements (for the same shell as in Figure 7) as functions of the centerline velocity, for n = 3.

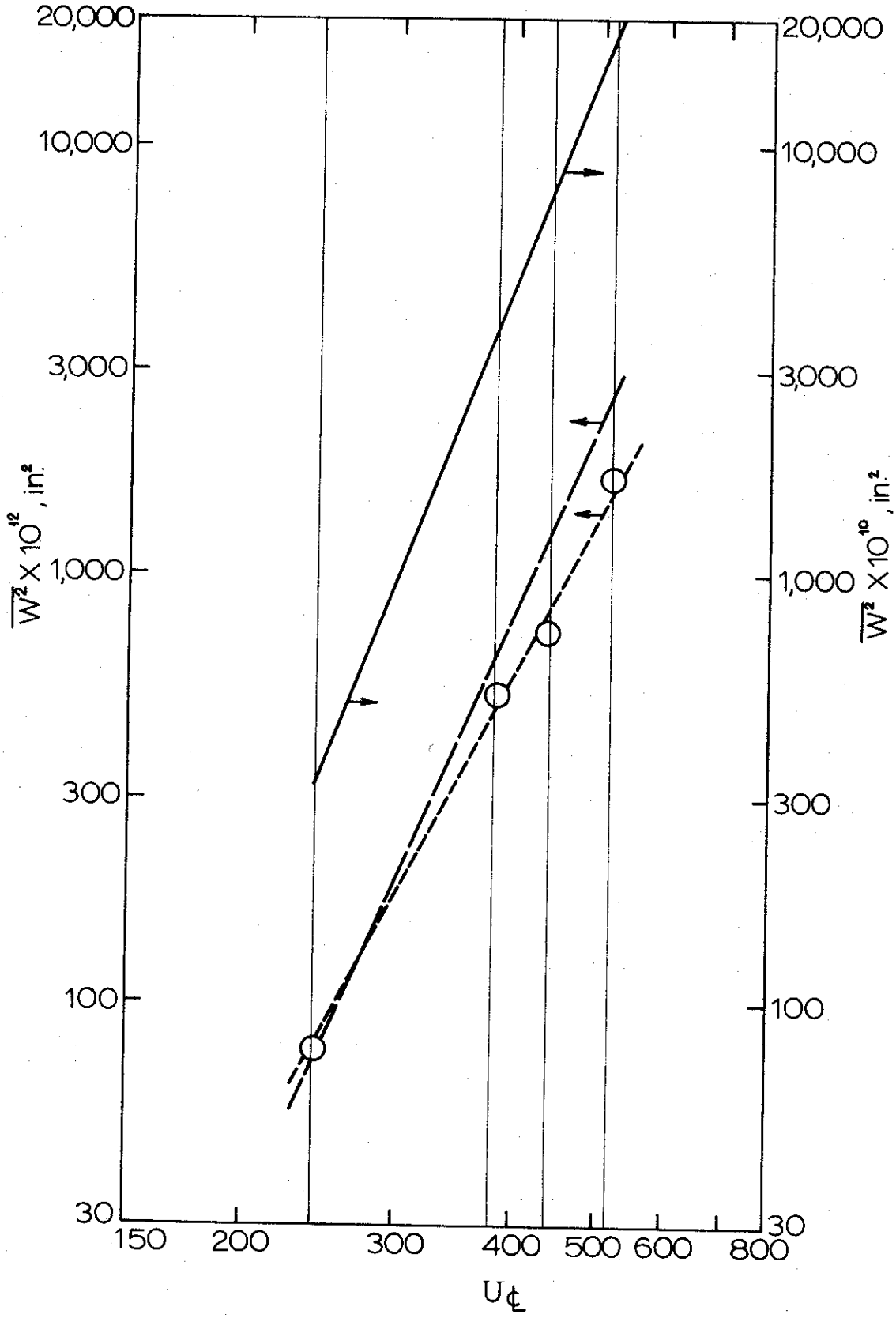

FIGURE 9 The mean square response of the radial displacement of a shell first studied by Clinch, as a function of the centerline velocity. -0--0- Clinch's experimental results for high-frequency response; — — — theoretical results obtained by this theory (with n = 2 to n = 6) for high-frequency response (93 - 1,000 Hz); ——— 'total' response obtained by this theory (with n = 2 to n = 6).

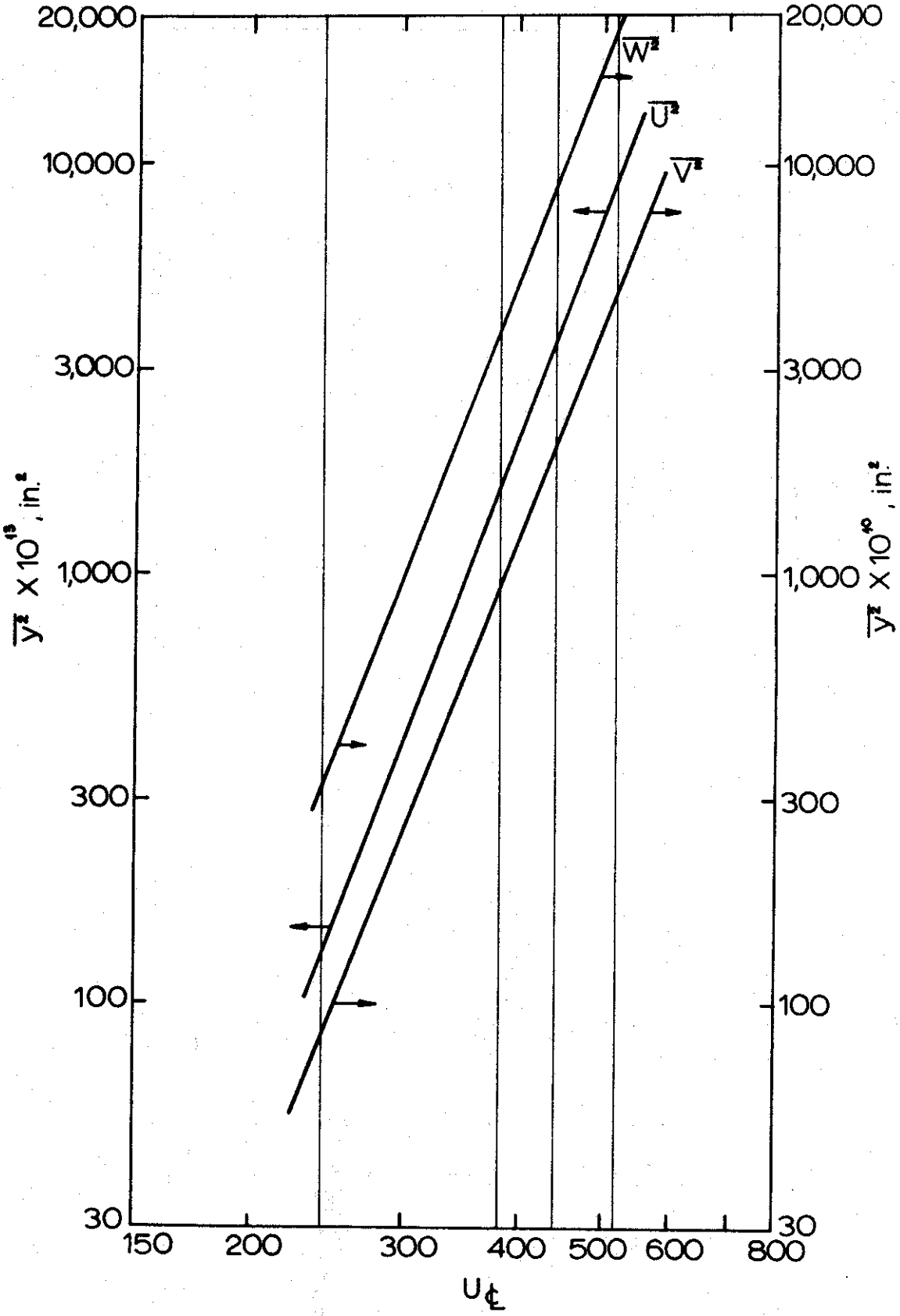

FIGURE 10 The mean square response of the radial, axial and circumferential displacements obtained by this theory (with n = 2 to n = 6) for the shell first studied by Clinch, ('total' response over whole frequency range).

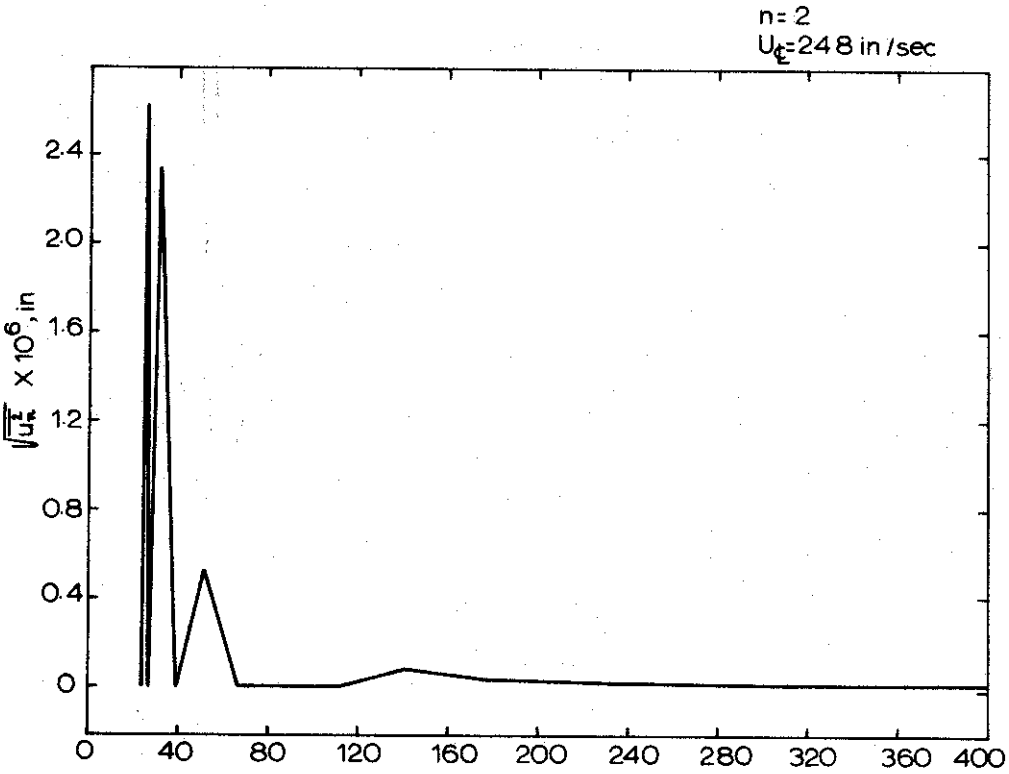
n = 2
U_ξ = 24.8 in/sec
$\sqrt{\overline{u_n^2}}$ X 10^6, in
2.4
2.0
1.6
1.2
0.8
0.4
0
0
40
80
120
160
200
240
280
320
360
400

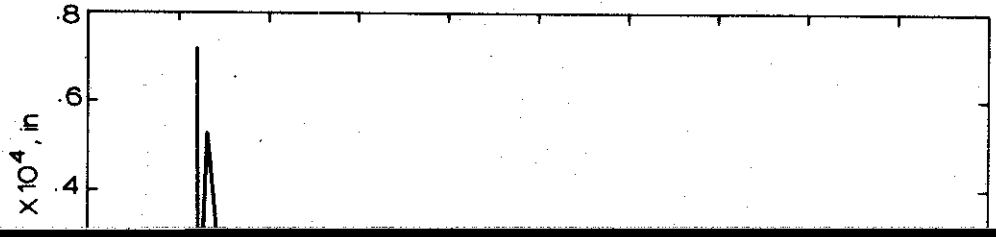
X 10^4, in
.8
.6
.4

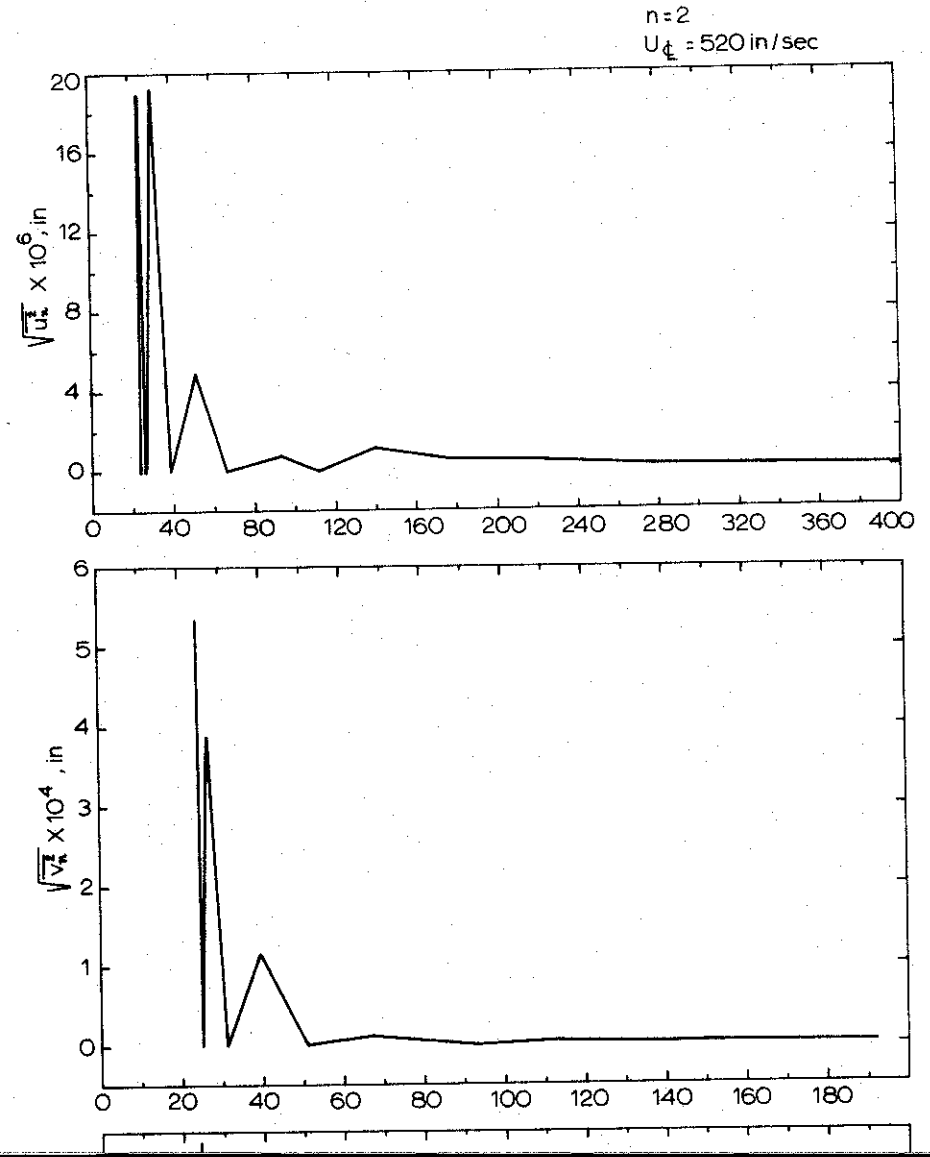
n = 2
$U_{\ell} = 520$ in/sec
$\sqrt{\overline{u_k^2}} \times 10^6$, in
0
4
8
12
16
20
0
40
80
120
160
200
240
280
320
360
400
$\sqrt{\overline{v_k^2}} \times 10^4$, in
0
1
2
3
4
5
6
0
20
40
60
80
100
120
140
160
180